COMPARING ALTERNATIVE DEVELOPMENTAL MODES: STRUCTURE AND GENE EXPRESSION IN THE OLFACTORY SYSTEM OF PLETHODONTID SALAMANDERS

By

Giuseppina Sole Lanzilli

A Thesis Presented to

The Faculty of California State Polytechnic University, Humboldt

In Partial Fulfillment of the Requirements for the Degree

Master of Science in Biology

Committee Membership

Dr. John Reiss, Committee Chair

Dr. Karen Kiemnec-Tyburczy, Committee Chair

Dr. Sharyn Marks, Committee Member

Dr. Amy Sprowles, Committee Member

Dr. Paul Bordeau, Program Graduate Coordinator

May 2024

ABSTRACT

COMPARING ALTERNATIVE DEVELOPMENTAL MODES: STRUCTURE AND GENE EXPRESSION IN THE OLFACTORY SYSTEM OF PLETHODONTID SALAMANDERS

Giuseppina Sole Lanzilli

The olfactory system of extant amphibians changes as the animal transitions from a fully aquatic to a terrestrial lifestyle at metamorphosis. Cellular morphology of the nose and expression patterns of olfactory genes in the nasal cavity have been examined for a variety of frogs and salamanders, but among plethodontid salamanders, molecular data are available only for *Plethodon shermani*. Using standard histology and micro-CT reconstruction, I investigated the structure of the olfactory organs of larvae, juveniles, and adults of six plethodontid species, with terrestrial, streamside, semiaquatic, and aquatic adults. The overall structure of the olfactory cavity was generally similar across species, but in *Desmognathus aureatus,* there was a great change in shape of the organ before and after metamorphosis, with a reduction of the epithelium not reported in other plethodontids.

At the molecular level, I used in situ hybridization to localize the expression of three G proteins ($G\alpha_{olf}$, $G\alpha_{o}$ and $G\alpha_{i2}$) and one cation channel (*TRPC2*). The expression of all the olfactory components did not vary between the juvenile and the adult life stages in terrestrial plethodontids. Generally, the main olfactory cavity expressed $G\alpha_{olf}$, the vomeronasal organ (VNO) expressed *TRPC2*, and $G\alpha_{o}$ was expressed in the whole

cavity. Expression of $G\alpha_{olf}$ in the VNO is absent in larvae but occurs in adults of some species. In direct-developing species, *TRPC2* is restricted to the VNO, while some biphasic species express it in the whole cavity. Thus, *TRPC2* appears to have a crucial role in chemoreception in all life stages and species.

ACKNOWLEDGEMENTS

Funding for this research was provided by the National Science Foundation (NSF) Grant (IOS #2050018, awarded to J. Reiss and K. Kiemnec-Tyburczy) and the California State University CSUBIOTECH 2023 Faculty-Graduate Student Research Collaboration Grant.

My first big thanks go to my advisors, Drs. John Reiss and Karen Kiemnec-Tyburczy. Thank you from the bottom of my heart for always supporting and encouraging me throughout my learning new techniques and my adapting to a different country, a different culture and different language. Thank you for being so welcoming and understanding since day one. If I had the chance for a fresh and promising start in my life, I owe it all to you. I am so grateful that the very first interaction I had here in the US was with two amazing people and researchers like you. Thank you for never giving up on me.

I would also like to thank the rest of my committee members: Dr. Sharyn Marks for being a great herpetology teacher and for first introducing me to the vast and amazing herpetological biodiversity in the U.S. and Dr. Amy Sprowles for training me in performing my first immunohistochemistry experiments and for granting me access to her lab supplies, including the fluorescence microscope. Thank you both for being so supportive and helpful towards my making progress in my Master's Program.

Another big thank you goes to my co-worker in this huge project Emily Gremling, for helping me collect some of my specimens in North Carolina, for taking care of them

afterwards and for performing her own experiments on my study species. I also thank Drs. Pamela and Richard Feldhoff (University of Louisville) for assistance with animal collection.

I would also like to acknowledge the other people who have worked and currently work in the animal room, Zachary Vegso, Jackie Patmore, Grace Laskey, Emmery Parker, Emily Gremling and Theo Ciemiewicz. Thank you so much for all the training and help in taking care of my salamanders.

I would like to thank Shea Alexander and Seanamae Adams for their incredible help with the 3D reconstructions of my focal species.

A huge thank you goes to the members of the "Fellowship of the Herps" Zachary Vegso, Emmery Parker, Marilyn Sandoval and Jekka Jones. Thank you for your invaluable friendship, love, and support, especially throughout my hardest times. I am so grateful for all the time we spent together herping, watching movies while eating yummy food, playing videogames, exchanging gifts, or just casually running into each other on campus and chatting for a little bit. I cherish all the forms of connection that I experienced with you amazing human beings. Thank you for being in my life, you will always hold a special place in my heart.

Thank you to all my acting, music, and circus friends, for helping me discovering and nurturing my creative mind, and for making me an actress and a soprano singer.

I would also like to thank all my friends in Italy, especially Nicola, Chicca, Diana and Ilenia, for never stopping supporting me even from 10,000 km away.

Finally, thank you to my parents. You will not be able to attend my defense in person, but I know you will be watching over me as the most precious angels. I love you. Thank you for making me who I am.

TABLE OF CONTENTS

LIST OF TABLES

LIST OF FIGURES

LIST OF APPENDICES

INTRODUCTION

Living amphibians are characterized by a wide diversity of developmental modes and ecologies (Duellman and Trueb 1994). Some of them are direct developers; they hatch as terrestrial juveniles that resemble adults. Others are biphasic species, meaning that they hatch in the water as larvae or tadpoles, and they undergo metamorphosis before becoming adults. Other species are paedomorphic, meaning that they retain larval characteristics (gills, for example) when they attain sexual maturity. In addition, adults of biphasic species can range from completely terrestrial to completely aquatic.

Both aquatic and terrestrial life history stages of many amphibians have a broad reliance on the sense of olfaction for social and reproductive purposes. For example, tadpoles use olfaction in kin recognition, feeding and predator avoidance, while adult anurans use olfaction in orientation/homing, mating, predation, and parental care in terrestrial habitats (Weiss et al. 2021). In lungless salamanders, both males and females use olfactory cues during courtship, in which olfactory pheromone delivery plays a key role (Arnold et al. 2017). The diversity in life histories and habitats, coupled with the extensive use of chemical communication in many groups, makes amphibians a useful system to study how these factors can influence the form and function of the olfactory system.

The Amphibian Olfactory System

From both morphological and molecular perspectives, the amphibian olfactory system is dual; it is composed of the main olfactory cavity (MOC) and the vomeronasal organ (VNO). In salamanders, the VNO is generally a lateral diverticulum off the MOC (Wirsig-Wiechmann et al. 2002; Eisthen 1997). In salamander larvae, both the MOC and VNO are used to smell underwater. In metamorphosed animals, however, the MOC can be used for both aquatic and terrestrial olfaction, as it detects volatile odorants (Reiss and Eisthen 2008). The VNO likely detects chemical signals like pheromones (low volatile, hydrophobic molecules) and water-soluble odorants in both aquatic and terrestrial environments (Dawley 1992, Baxi et al. 2006). Sensory neurons in the olfactory epithelium of the whole nasal cavity (both the MOC and VNO) have axonal projections to the olfactory bulb of the brain.

The sensory cells embedded in the epithelia lining the MOC and VNO express G-Protein Coupled Receptors (GPCRs) that bind the molecular odorant ligands required to elicit the appropriate cellular olfactory response. The four major families of GPCRs known to bind olfactory ligands are Olfactory Receptors (ORs), Trace Amine-Associated Receptors, Vomeronasal Type 1 Receptors (V1Rs) and Vomeronasal Type 2 Receptors (V2Rs) (Fleischer et al. 2009). Once a GPCR is activated, the signal transduction pathway converts the molecular signal into an electrical one via the opening of specific ion channels in the cell membrane, causing olfactory neuron depolarization (Buck and Axel, 1991). One of these channels is the Transient Receptor Potential Cation channel,

subfamily C, member 2 (*TRPC2*), a cation channel belonging to the transient receptor potential family of ion channels. This ion channel colocalizes with the V1R *and* V2R families of receptors (Kiselyov et al. 2010), and it is involved in pheromone detection in the VNO of mammals (Venkatachalam and Montell 2007).

Each type of GPCR is associated with a specific subclass of G protein, each of which itself has three subunits (Duc et al. 2015). The ORs are known to be associated with the G protein subunit $G\alpha_{olf}$ (*olf* stands for olfaction), which is specifically expressed in the olfactory sensory neurons (Buck and Axel 1991). Trace Amine-Associated Receptors are expressed in sparse, nonoverlapping subsets of olfactory sensory neurons within the main olfactory epithelium, and they are associated with $G\alpha_{olf}$ as well (Liberles and Buck 2006). The V1Rs are associated with $G\alpha_{i2}$ (*i* stands for inhibition), which has been detected in most types of cells (Dulac and Axel 1995). The fourth GPCR family, V2R, is associated with $G\alpha_{o}$ (Herrada and Dulac 1997).

Patterns of GPCR and G protein expression are of interest because they likely reflect functional differences in the olfactory sensitivity of an animal. In addition, expression patterns are variable across vertebrate lineages. In *Mus musculus*, a fully terrestrial mammal, $G\alpha_{olf}$ and ORs are found expressed exclusively in the MOC, while V1Rs, V2Rs and the ion channel *TRPC2* are expressed only in the VNO (Liman and Dulac 2007; Fleischer et al. 2009). On the other hand, differences in GPCR and G protein expression profiles have been reported in a small number of other taxa (frogs, salamanders, newts) with life stages that occur in terrestrial or aquatic environments. For example, aquatic adult clawed frogs express *TRPC2* in parts of the MOC (Sansone et al.

2014) and aquatic phase newts express $G\alpha_{olf}$ in the VNO (Nakada et al. 2014). It has been hypothesized that expression variation in the nasal cavity corresponds to differences in life history stage (larvae vs. adults) and habitats (terrestrial vs. aquatic), but limited sampling has made it challenging to assess broad patterns across lineages.

Focal Species

Plethodontid salamanders (Family Plethodontidae) represent the most diverse and largest family of salamanders (Wake 2012), with more than 450 species described. Their range extends from southern Canada to northern Bolivia and eastern Brazil in the Americas, to Europe (mainland France, northern Italy, Sardinia) and the Korean peninsula (Stebbins and McGinnis 2018), and they exhibit a great diversity in developmental modes (direct development, biphasic life cycle, neoteny/paedomorphosis). All plethodontids are lungless, and they breathe through their skin, which is thin, smooth, and moist. A fundamental feature of members of this family is the presence of nasolabial grooves, which are depressions that go from the nostrils to the edge of the upper lip, and function to transport waterborne odorants from the substrate to the nose (Dawley and Bass 1989; Stebbins and McGinnis 2018).

The primary focus of my research is the plethodontid genus *Desmognathus* (Dusky Salamanders), containing up to 49 candidate species based on recent ecogeographic sampling (Pyron et al. 2022). The species belonging to this genus display both direct-developing and biphasic life histories, despite convincing evidence that the genus is monophyletic (Fig. 1). Recent phylogenetic studies revealed that direct

development is the ancestral life history of this clade and that a biphasic life history was reacquired within *Desmognathus* (Chippindale et al. 2004; Beachy et al. 2017). The variation of life history strategies and ecologies found in the genus *Desmognathus* may influence olfactory form and function and led me to choose this genus for my research (Table 1).

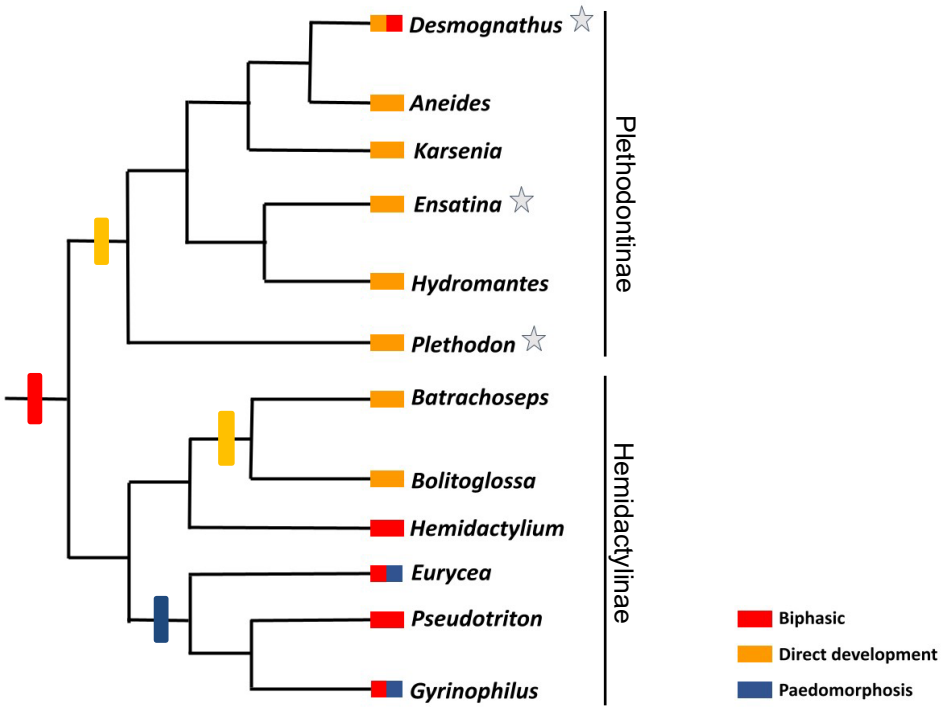

Figure 1. *Simplified phylogeny of* Plethodontidae *(adapted from Bonett et al. 2014). Biphasic development with larvae is assumed to be the ancestral state for the family, with direct development derived twice independently. Re-evolved biphasic life history occurs in some species of* Desmognathus*, and paedomorphosis occurs in some species of* Gyrinophilus *and* Eurycea*. Stars indicate the genera I sampled.*

The species I selected were *D. wrighti* (a direct developer), which is likely the earliest diverging species in the *Desmognathus* phylogenetic tree (Pyron et al. 2020), and

three biphasic species: *D. ocoee*, *D. amphileucus* (formerly *D. quadramaculatus*) and *D. aureatus* (formerly *D. marmoratus*) (Fig. 2). Some of the biphasic species are more aquatic as adults than others. Body size, length of the larval period and habitat also vary considerably among them (Bruce 2005; Table 1). Notably, metamorphosed adults of *D. aureatus* display a profound reduction of the olfactory epithelium of the MOC compared to other biphasic species in the genus (Dawley 2017) and they also show a paedomorphic retention of lateral line pores (sensu Hilton 1947), which constitute a sensory organ used for detecting movements, sensing vibration and pressure.

Table 1. *General characteristics of life history, habitat, snout to vent length (SVL) at metamorphosis, and larval period length (if applicable) of focal species (taken from Bruce 2005).*

	Life History	**Habitat**	**Metamorphosis SVL (mm)**	**Larval period (mo)**
D. amphileucus	Biphasic	Semiaquatic	35 - 54	34 - 47
D. aureatus	Biphasic	Aquatic	25 - 38	10 - 20
D. ocoee	Biphasic	Streamside	11 - 15	9 -10
D. wrighti	Direct developing	Terrestrial	N/A	N/A
E. eschscholtzii	Direct developing	Terrestrial	N/A	N/A
P. shermani	Direct developing	Terrestrial	N/A	N/A

I used *Plethodon shermani* and *Ensatina eschscholtzii* (both also in the plethodontid subfamily Plethodontinae) as outgroups of *Desmognathus* (Fig. 1). I included *P. shermani* as an outgroup for my study specifically because of the extensive research that has been done on pheromonal communication in this species (Wirsig-Wiechmann et al. 2002, 2006; Arnold et al. 2017; Wilburn et al. 2017) and the availability of previous work on olfactory and vomeronasal gene expression (Kiemnec-Tyburczy et al. 2012). *Ensatina eschscholtzii* was selected as the second direct-

developing outgroup species, to give me the ability to assess differences in structure and gene expression patterns between two direct-developing species outside *Desmognathus*.

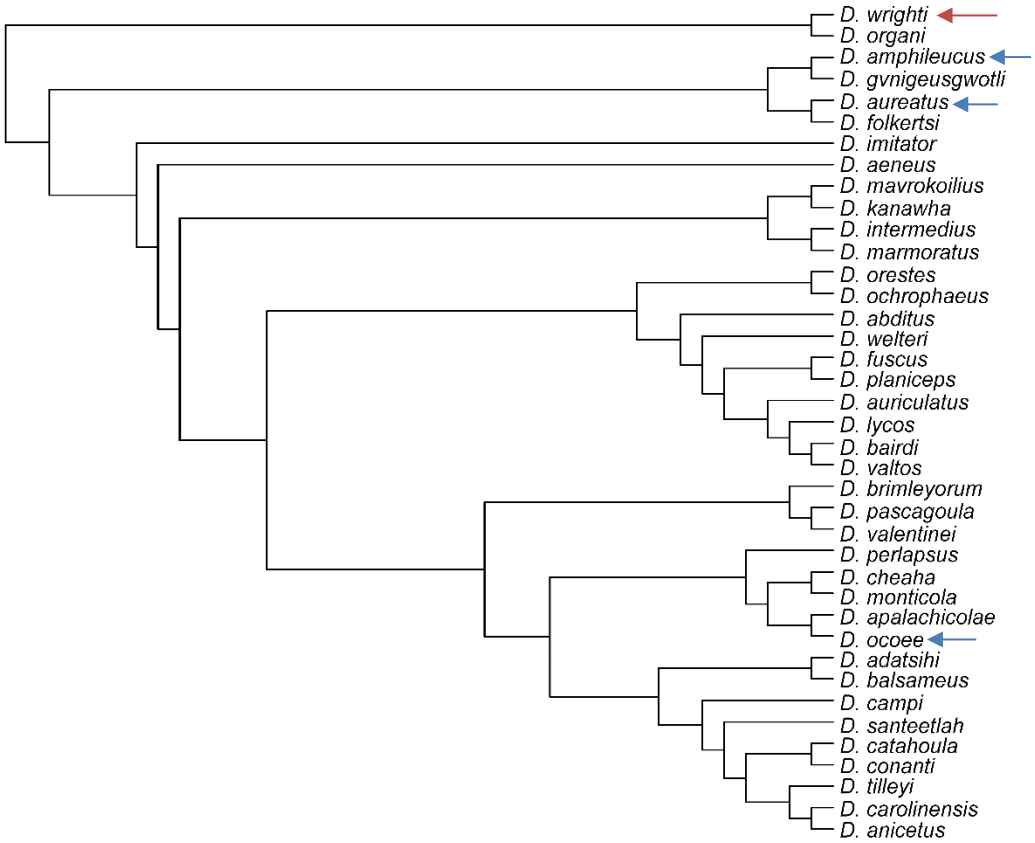

Figure 2. Desmognathus *phylogeny showing the relationships between the 39 currently described* Desmognathus *species (adapted from Pyron et al. 2022). Arrows show the species that I sampled. Red arrows indicate direct developers, blue arrows indicate biphasic species.*

Research Objectives

The goal of my thesis was to investigate the structure of the olfactory organ, as well as to describe the localization patterns of gene expression in the sensory cells of the

MOC and the VNO of six species of plethodontid salamanders, including larval, juvenile, and adult life stages, to characterize the olfactory system in this family. I focused on the expression patterns of three G protein alpha subunits and the *TRPC2* ion channel in the sensory cells of the MOC and the VNO. I examined the localization of G proteins and *TRPC2* because they are considered proxies for the location of expression of different classes of olfactory receptors, and thus I could infer broad patterns of GPCR family expression from my results. Based on previous observations from other taxa, I developed three predictions about the structure and expression in the olfactory systems of my focal species:

- I predicted that animals with similar ecologies would have similar nasal cavity morphologies (e.g., a sac-like shape in terrestrial juveniles and adults of all genera and a flatter olfactory cavity in highly aquatic juveniles and adults of biphasic species).
- I predicted that the expression pattern of my selected olfactory components would be conserved in life stages with similar ecologies (e.g., in aquatic larvae and aquatic adults because they do not change habitat throughout their life).
- I predicted that expression of olfactory genes would be different in the larval stages versus adult stages of my biphasic species with terrestrial adults, related to a change in habitat between these two life stages (water vs. land).

MATERIALS AND METHODS

Specimen Collection and Identification

I collected multiple life stages of six species of plethodontid salamanders from natural populations during June-August 2021 and June 2022 (Table 2). I collected adult *E. eschscholtzii* in northern California, while I collected the other five species in southwestern North Carolina (see Appendix A for the life stage at the time of collection versus time of euthanasia for each specimen). Animals were collected with a California Scientific Collecting permit (S-200260005-20362-001) or in accordance with the Amphibian and Reptile Possession Policy set by the North Carolina Wildlife Resources Commission.

In addition to *E. eschscholtzii*, I sampled *Plethodon shermani* (juveniles and adults) and four species of *Desmognathus*: *D. wrighti* (adults), *D. ocoee* (adults), *D. aureatus* (larvae and adults) and *D. amphileucus* (larvae and adults). Initial identification in the field was based on morphological characters (such as head shape and gill color). Due to recent changes in the taxonomy of this genus, I also used a molecular marker to genetically identify each specimen. I collected tail tips from each specimen at the time of euthanasia and stored them in 100% ethanol. I extracted genomic DNA using a DNeasy Blood and Tissue kit (Qiagen, Valencia, CA, Catalog #69504) following the manufacturer's protocol. I then amplified a fragment of the cytochrome *b* locus using the PCR conditions and cycling parameters described previously (Beamer and Lamb 2008). Purified PCR products were sent to Eurofins Genomics (Louisville, KY) for Sanger

sequencing. The resulting sequences were compared to reference sequences that are publicly available on NCBI GenBank.

Animal Euthanasia

I anesthetized the animals by placing them in a solution of 1:1000 Tricaine-sulfonate (MS-222, Western Chemical) buffered to pH 7.4 with sodium bicarbonate. After 15-20 minutes and loss of the righting reflex, I placed each animal under the dissecting microscope to measure the total length (TL) and snout to vent length (SVL) and determine sex (by dissection and observation of gonads). I removed the heads and/or heads and torsos of the animals by decapitation and preserved them appropriately for specific techniques as detailed below. All animal procedures were approved by the Cal Poly Humboldt Institutional Care and Use Committee (IACUC Protocol 2022B40-A).

Table 2. *Collection sites names and coordinates for each species and stage.*

	Collection Site Name	Collection Site Coordinates
***Ensatina eschscholtzii* adults**	Arcata Community Forest, Arcata, Humboldt County, CA	40.875498, -124.072813
***Plethodon shermani* adults**	Wayah Bald (Wilson's Lick), Macon County, NC	35.067756, -83.519050
***Plethodon shermani* juveniles**	Long Branch Trail, near Standing Indian Campground, Macon County, NC Wayah Bald - Wilson's Lick, Macon County, NC	35.074127, -83.514718 35.067756, -83.519050
***Desmognathus wrighti* adults**	Standing Indian Gap, NC Long Branch Trail, near Standing Indian Campground, Macon County, NC	35.079189, -83.529415 35.27697, -82.80778
***Desmognathus ocoee* adults**	Park Gap, Nantahala Mountains- Blue Ridge, Macon County, NC Rock Gap - Nantahala National Forest, Macon County, NC	35.074407, -83.537621 35.099458, -83.523499
***Desmognathus amphileucus* adults**	Lower Ridge Trail, Standing Indian Campground, Macon County, NC Ball Creek Road near Coweeta Lab, Macon County, NC East Fork Creek, Blue Valley, Macon County, NC	35.062790, -83.542641 35.057043, -83.431273 35.018484, -83.245067
***Desmognathus amphileucus* larvae**	HBS Falls Creek, Macon County, Highlands, NC	35.054088, -83.189375
***Desmognathus aureatus* adults**	East Fork Creek, Macon County, Blue Valley, NC	35.018484, -83.245067
***Desmognathus aureatus* larvae**	East Fork Creek, Macon County, Blue Valley, NC	35.018484, -83.245067

Standard Histology

I fixed each head (one animal per species and stage) in 10% neutral buffered formalin (NBF) overnight, decalcified in RDO Rapid Decalcifier (Apex Engineering, Aurora, IL, Catalog #RDO01) for 2 hours, dehydrated by immersing the head in a series of ethanol solutions of increasing concentration to 100% ethanol, placed in toluene, and finally embedded in paraffin. After paraffin block trimming, I sectioned the head at 10

μm with a rotary microtome. I placed the resulting sections on slides after applying Haupt's solution and 3% formalin on them, and then I placed the slides on a slide warmer for drying. Once the slides were dried, I stained the tissue sections following a hematoxylin and eosin standard protocol (Humason 1979), followed by coverslipping and mounting sections with Permount mounting medium (Fisher Scientific, Fair Lawn, New Jersey, Catalog #SP15-100). I examined the slides on a Nikon Eclipse E400 microscope and photographed using a Canon EOS digital camera. See Appendix A for the number of animals euthanized for this procedure.

MicroCT Scanning and 3D Reconstruction

Once euthanized, I bisected the body of each animal and placed the anterior half in 10% NBF for at least a day and then stained with 1% Lugol's solution (Gignac et al. 2016). All heads were submerged in Lugol's solutions for at least two days, but some up to a week (the duration of incubation depended on the head size with larger heads requiring longer incubation). Once fully stained, I placed the animal in 50% ethanol and then I scanned the head using a Nikon XTH-225 MicroCT scanner. Image stacks were processed for segmentation of olfactory structures and their 3D reconstruction using the software 3D Slicer, version 5.6.1 (slicer.org). I outlined both the MOC and the VNO on each reconstruction for each species and life stage. I scanned one animal per species and life stage.

In Situ Hybridization

I used in situ hybridization to detect the presence of mRNA in olfactory neurons in the salamander nasal cavity (Kiemnec-Tyburczy et al., 2012). Because of the expected genetic divergence in the olfactory genes across the three genera, I produced a separate set of gene-specific probes for each species. The first step in the process was to isolate the sequences of the homologs from the olfactory genes (TRPC2, $G\alpha_{olf,}$ $G\alpha_{o}$ and $G\alpha_{i2}$) from every species so that they could be used as templates for cRNA probe production.

I first harvested the olfactory tissue of a single adult of all my focal species and stored it in RNAlater (Invitrogen, Carlsbad, CA, Catalog #AM7020) at -20°C until RNA extraction (Appendix A). I performed RNA extraction on each of the tissues using a silica column-based purification kit (RNAqueous-4PCR Total RNA Isolation Kit, Invitrogen, Catalog #400793). I synthesized the complementary DNA (cDNA) from RNA from each species using the protocol provided with the RevertAid First Strand cDNA Synthesis Kit (ThermoFisher Scientific, Vacaville, CA, Catalog #K1622). I subsequently used these cDNAs as templates to amplify the olfactory-related genes from all six species using degenerate PCR primers with DreamTaq DNA polymerase (ThermoFisher Scientific, Catalog #EP1701) with various conditions (see Appendix B for cycling conditions, sequences of primers used for each species, and gene fragment lengths). I prepared amplicons of the predicted size for sequencing using Sanger DNA sequencing (Eurofins Genomics, Louisville, KY) and once the amplicon was verified to be the correct locus, each PCR product and subcloned into the TA cloning site of the pGEM-Teasy cloning

vector, which is flanked by SP6 and T7 promoters (pGEM-Teasy; Promega Corporation, Madison, WI, Catalog #A1360). The successful insertion of each PCR product was verified by Sanger sequencing of every plasmid (nucleotide sequences available by request). Digoxigenin (DIG)-labeled sense and antisense riboprobes were generated by in vitro transcription using either SP6 or T7 RNA polymerase (ThermoFisher Scientific). The riboprobes were purified using lithium chloride and ethanol and stored at -80°C until used for hybridization experiments.

I fixed the heads of every animal in 4% paraformaldehyde (PFA)/1X phosphate-buffered saline (PBS; pH.7.4) overnight, decalcified in 10% EDTA in DEPC water for 24-72 hours (time varied based on size of animal's head) and cryoprotected in 30% sucrose in DEPC water once the tissue was fully decalcified (see Appendix A for specimen information). The heads were embedded in OCT embedding medium (Fisher Scientific, Hampton, NH), sectioned in the transverse plane at 16 µm with a cryostat (International Equipment Company, Model CTD Harris-Cryostat), and mounted on poly-L-lysine coated slides. Slides were prepared by smearing three drops of 0.1% poly-L-lysine (Sigma-Aldrich, St. Louis, MO, Catalog #P8920) onto super frost plus slides (Fisher Scientific, Hampton, NH, Catalog #22-037-246) and drying at 60°C for at least an hour before tissue was adhered to them.

I carried out the hybridization of probes using a protocol modified from Butler et al. (2001). The sections were rinsed twice with 2XSSPE, incubated them with 20 units of proteinase K for 30 min and rinsed again in SSPE. I then refixed the sections in 4% paraformaldehyde in PBS for 10 min, incubated with 0.2 M HCl for 15 min, rinsed with

SSPE and incubated with 0.1 M triethanolamine (Sigma-Aldrich, St. Louis, MO, Catalog #T1502-250G), pH 8.0, for 5 min. After two sequential additions of acetic anhydride, I incubated the slides with a hybridization solution containing 5 ng/µL cRNA probe, 50% formamide, 1% blocking reagent (Roche Diagnostics, Catalog #11 096 176 001), 5X SSC (Fisher Scientific, Catalog #AM9763), 5 mM EDTA, 0.5 mg/mL Torula RNA (Sigma-Aldrich, Catalog #83850), 0.1 mg/mL heparin (Fisher Scientific, Catalog #BP2425), 0.1% Tween-20 (Sigma-Aldrich, Catalog #P1379-25ML) at 60°C for 2 hours. The probe hybridization was performed using both antisense and sense probes at 63°C for 15 hours. Probe concentrations depended on the size of the animal. For larger heads, I used 15 ng/µL and 20 ng/µL probe concentrations, while for smaller heads, I used 5 ng/µL and 10 ng/µL probe concentrations (Table 3). As for control probes, I used the higher concentration of each specific probe on every run.

After the overnight hybridization, I incubated the sections with 5 µg/mL RNAse A (Sigma-Aldrich, Catalog #R5000) for 30 min at 37°C, incubated in 50% formamide (Avantor, Visalia, CA, Catalog #EM-4610) for 30 min at 60°C and rinsed three times with a buffer solution containing 100 mM Tris (pH 7.5), 5 M NaCl and DEPC water. Then, I incubated the sections for 2 hours in a blocking buffer containing 100 mM Tris (pH 7.5), 5 M NaCl and blocking reagent (Roche Diagnostics, Catalog #11 096 176 001). Next, I incubated the slides with alkaline phosphatase-conjugated antiDIG Fab fragment antibody (Roche Diagnostics, Catalog #11093274910) for 1 hour, washed them three times with a buffer solution containing 100 mM Tris (pH 7.5), 5 M NaCl and DEPC water, and equilibrated them in alkaline phosphatase buffer for 10 min before incubating

the slides in BM purple chromogenic substrate (Roche Diagnostics, Catalog #11442074001) for 15 hours. I stopped the reaction with a solution of MEMFA fixative in DEPC water for 40 min. I dehydrated the tissue with two washes of 99% histological grade isopropanol, and I mounted the slides using a mounting medium, VectaMount® Express (Vector Laboratories Inc. Newark, CA, Catalog #H-5700) and coverslipped them, following the protocol provided by the manufacturer. After the slides were dried, I observed the staining pattern for the G proteins and the *TRPC2* receptor across the olfactory organ using a Nikon Eclipse E400 microscope and photographed using a Canon EOS digital camera.

Table 3. *Number of animals and concentrations of cRNA probes used for in situ hybridization on different species and life stages.*

Species	Number of animals	$G\alpha_{olf}$	*trpc2*	$G\alpha_{o}$	$G\alpha i_2$
***E. eschscholtzii* adults**	2	5-10 ng/µl	5-10 ng/µl	15-20 ng/µl	15-20 ng/µl
***P. shermani* juveniles**	2	5-10 ng/µl	5-10 ng/µl	15-20 ng/µl	15-20 ng/µl
***D. wrighti* adults**	1	10-15 ng/µl	10-15 ng/µl	15-20 ng/µl	15-20 ng/µl
***D. ocoee* adults**	1	5-10 ng/µl	5-10 ng/µl	15-20 ng/µl	15-20 ng/µl
***D. amphileucus* adults**	1	5-10 ng/µl	5-10 ng/µl	5-20 ng/µl	15-20 ng/µl
***D. amphileucus* larvae**	2	10-15 ng/µl	5/10 ng/µl	5-20 ng/µl	15-20 ng/µl
***D. aureatus* adults**	1	5-10 ng/µl	5-10 ng/µl	5-20 ng/µl	15-20 ng/µl
***D. aureatus* larvae**	1	10-15 ng/µl	10-15 ng/µl	5-20 ng/µl	15-20 ng/µl

RESULTS

General Morphology of Olfactory Organ of Direct-Developing Plethodontids

I observed a similar organization of the olfactory cavity in all my terrestrial, direct-developing species and life stages: *Ensatina eschscholtzii* adult (Fig. 3A-F), *Plethodon shermani* adult (Fig. 4A-H), *Plethodon shermani* juvenile (Fig. 5A-F), and *Desmognathus wrighti* adult (Fig. 6A-I). Generally, the olfactory organ of the terrestrial plethodontids extends from the external naris at its rostral end to the internal naris (choana) at its caudal end, where it meets with the buccal cavity. At the level of the external naris the MOC can be seen surrounded by a thick layer of olfactory epithelium (e.g., Fig. 3C). The MOC is significantly wider midway back through the organ, and at this level it is possible to see the VNO as a lateral diverticulum (e.g., Fig. 3D). From this level towards the posterior end, both the MOC and the VNO become more dorso-ventrally compressed, while being surrounded by a very thin layer of epithelial cells. Respiratory (non-sensory) epithelium lies at the zone of separation between the two regions of the nose (MOC and VNO), while the rest is all olfactory epithelium (e.g., Fig. 3E, F).

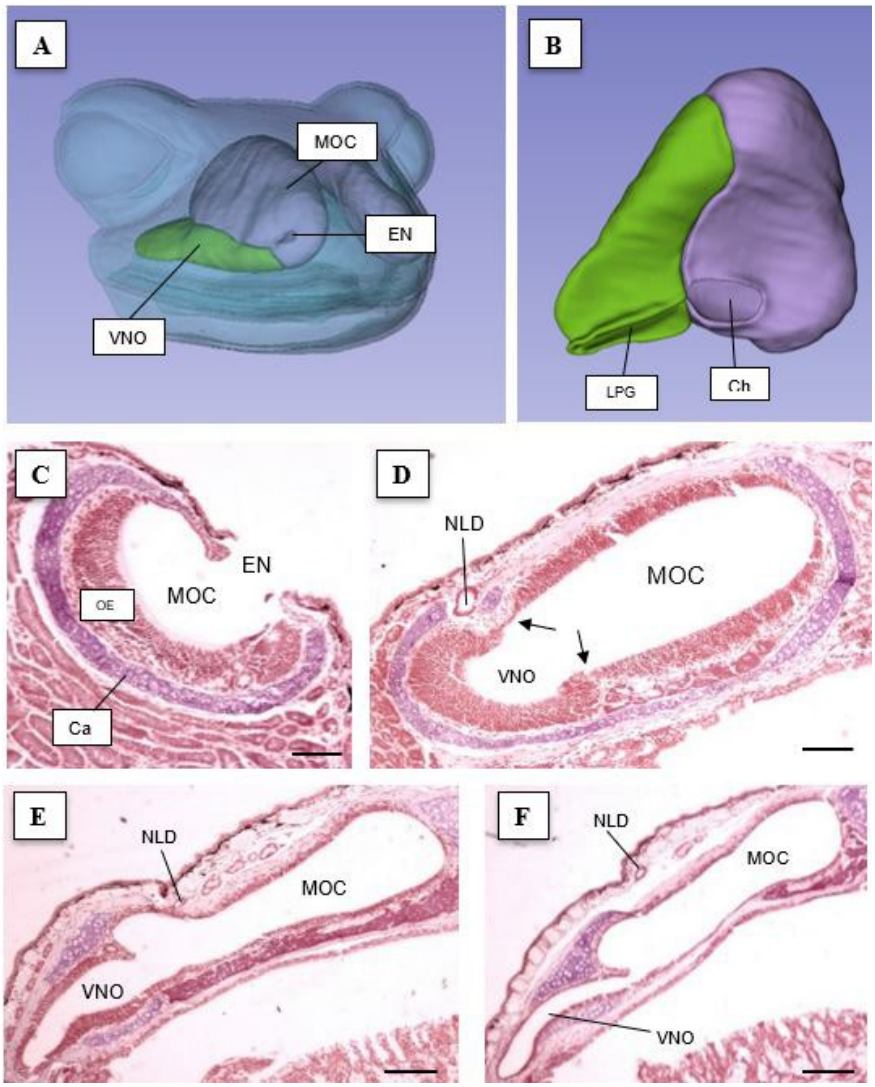

Figure 3. *Tridimensional reconstruction and light micrographs of transverse sections through the adult olfactory organ of* Ensatina eschscholtzii. ***A:*** *Anterolateral view of the 3D reconstruction of both olfactory organs. The MOC (main olfactory epithelium) is purple, the VNO (vomeronasal organ) is light green.* ***B:*** *Ventral view of the 3D reconstruction of the right olfactory organ (Ch: choana; LPG: lateral palatal groove). The MOC is purple, the VNO is light green.* ***C:*** *The external nares (EN), the beginning of the main olfactory cavity (MOC), the olfactory epithelium surrounding it (OE) and the cartilage layer (Ca).* ***D:*** *The MOC and the vomeronasal organ (VNO); the nasolacrimal duct (NLD) is also visible. The arrows indicate regions of respiratory (non-sensory) epithelium.* ***F:*** *Both the MOC and the VNO appear dorso-ventrally compressed, and the OE is thinner. Scale bar (C): 100 µm; scale bar (D, E, F): 200 µm.*

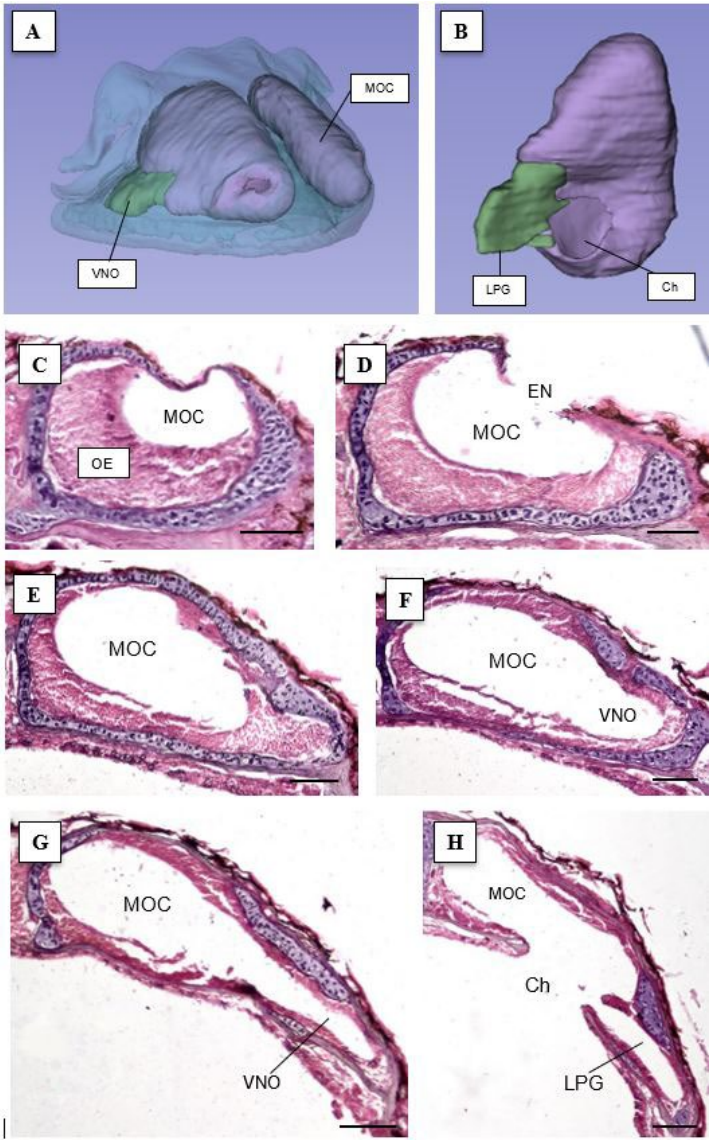

Figure 4. *Tridimensional reconstruction and light micrographs of transverse sections through the juvenile olfactory organ of* Plethodon shermani. ***A:*** *Anterolateral view of the 3D reconstruction of both olfactory organs. MOC is shown in purple, VNO in light green.* ***B:*** *Ventral view of the 3D reconstruction of both olfactory organs. MOC is shown in purple, VNO is in light green.* ***C:*** *The thick olfactory epithelium (OE) and the cavity posterior to the external nares.* ***D:*** *External nares (EN) and the main olfactory cavity (MOC).* ***E, F:*** *The MOC and the vomeronasal organ (VNO) appear broader, while the OE is thinner.* ***G:*** *both the MOC and VNO appear narrow.* ***H:*** *At the very back of the nose, the MOC transitions into the choana (Ch) and the VNO transitions into the lateral palatal groove (LPG). Scale bar (C, D, E, F): 200 µm; scale bar (G, H): 150 µm.*

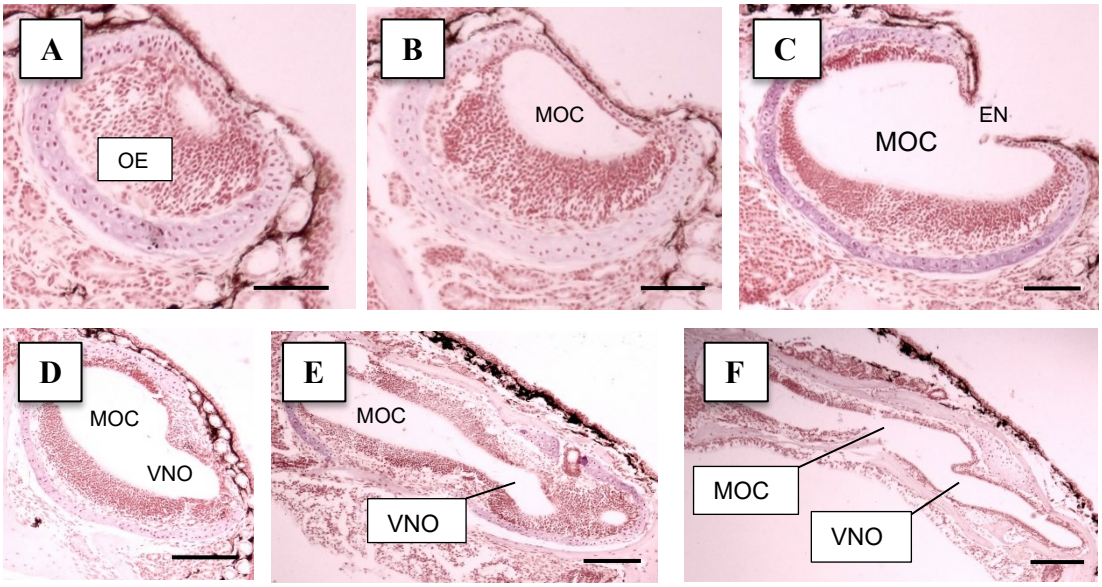

Figure 5. *Light micrographs of transverse sections through the adult olfactory organ of* Plethodon shermani. ***A, B:*** *The thick olfactory epithelium (OE) and the main olfactory cavity MOC.* ***C:*** *The MOC at the level of the external nares (EN).* ***D:*** *The MOC and the vomeronasal organ (VNO) are broad.* ***E, F:*** *Both the MOC and the VNO are more dorso-ventrally compressed towards the back of the nose. Scale bar (C): 75 µm; scale bar (D): 150 µm; scale bar (E, F): 300 µm.*

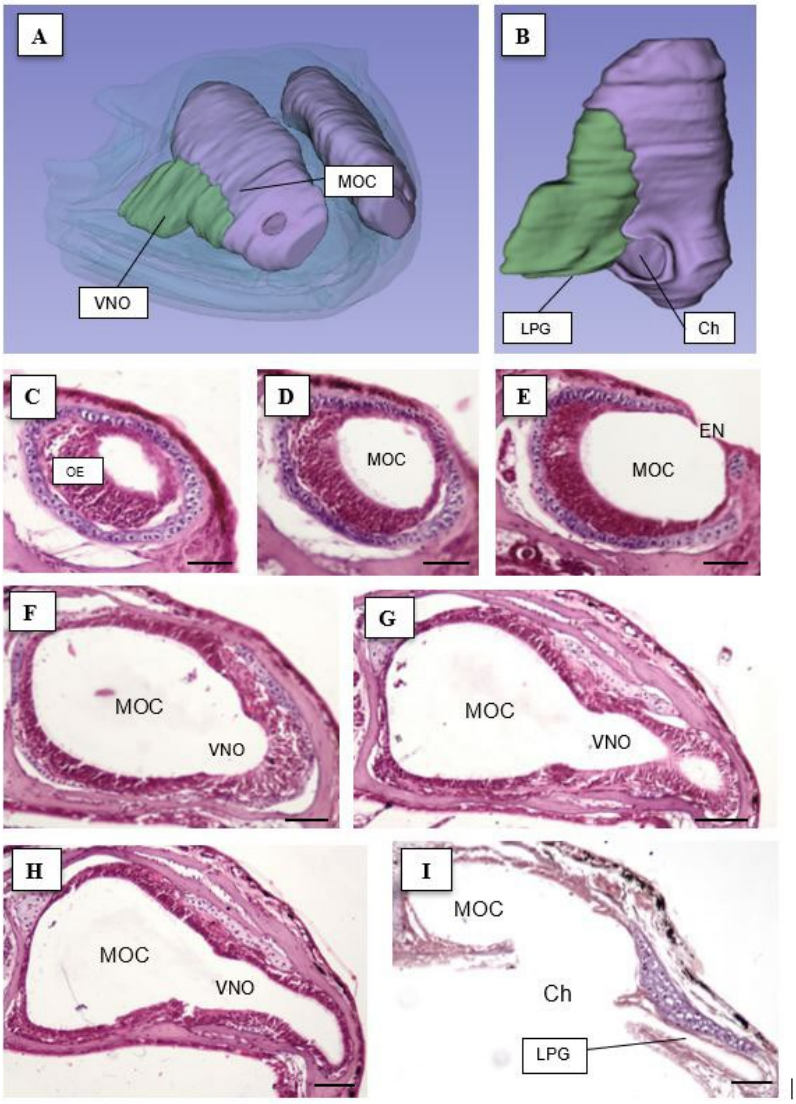

Figure 6. *Tridimensional reconstruction and light micrographs of transverse sections through the adult olfactory organ of* Desmognathus wrighti. ***A:*** *Anterolateral view of the 3D reconstruction of both olfactory organs. MOC is shown in purple, VNO is light green.* ***B:*** *Ventral view of the 3D reconstruction of both olfactory organs. MOC is shown in purple, VNO is in light green.* ***C:*** *Thick layer of olfactory epithelium (OE) in the main olfactory cavity (MOC).* ***D:*** *External nares (EN) and MOC.* ***E, F, G, H:*** *The MOC and the vomeronasal organ (VNO).* ***I:*** *Lateral palatal groove (LPG) and the MOC at the level of the choana (Ch). At this level of the nose, the olfactory epithelium was very thin, and some was lost artifactually. Scale bar (C, D, E, F, G, H): 75 µm; scale bar (I): 100 µm.*

General Morphology of the Olfactory Organ of Biphasic Plethodontids

I observed several notable differences in morphology of the adults of biphasic species. The olfactory organ of adult *D. ocoee* (Fig. 7A-H), has the same overall organization as the terrestrial direct-developing species. But in *D. amphileucus* adults, the epithelium is organized similarly to *D. ocoee*, but the overall olfactory organ is significantly flatter (Fig. 8A-G). In larval *D. aureatus* (Fig. 9A, B), the olfactory cavity appears to be elongated and tubular. It is noteworthy that the epithelium surrounding the cavity is thick all the way along the length of the organ, rather than thinning posteriorly (Fig. 9). The MOC begins posterior to the external nares (Fig. 9C), with the VNO extending as a small diverticulum from the central region of the MOC (Fig. 9D, E). Only the MOC extends to the very back of the nose, where it opens to the buccal cavity through the choana (Fig. 9F).

In the olfactory organ of *D. aureatus* (Fig. 10A-F), the whole cavity's shape (both MOC and VNO) is quite flat. From the sections available, the extremely thin olfactory epithelium already reported by Dawley (2017) could be seen. Interestingly, it was not easy to identify a clear distinction between the two regions (MOC versus VNO) of the nose (Fig. 10A, B).

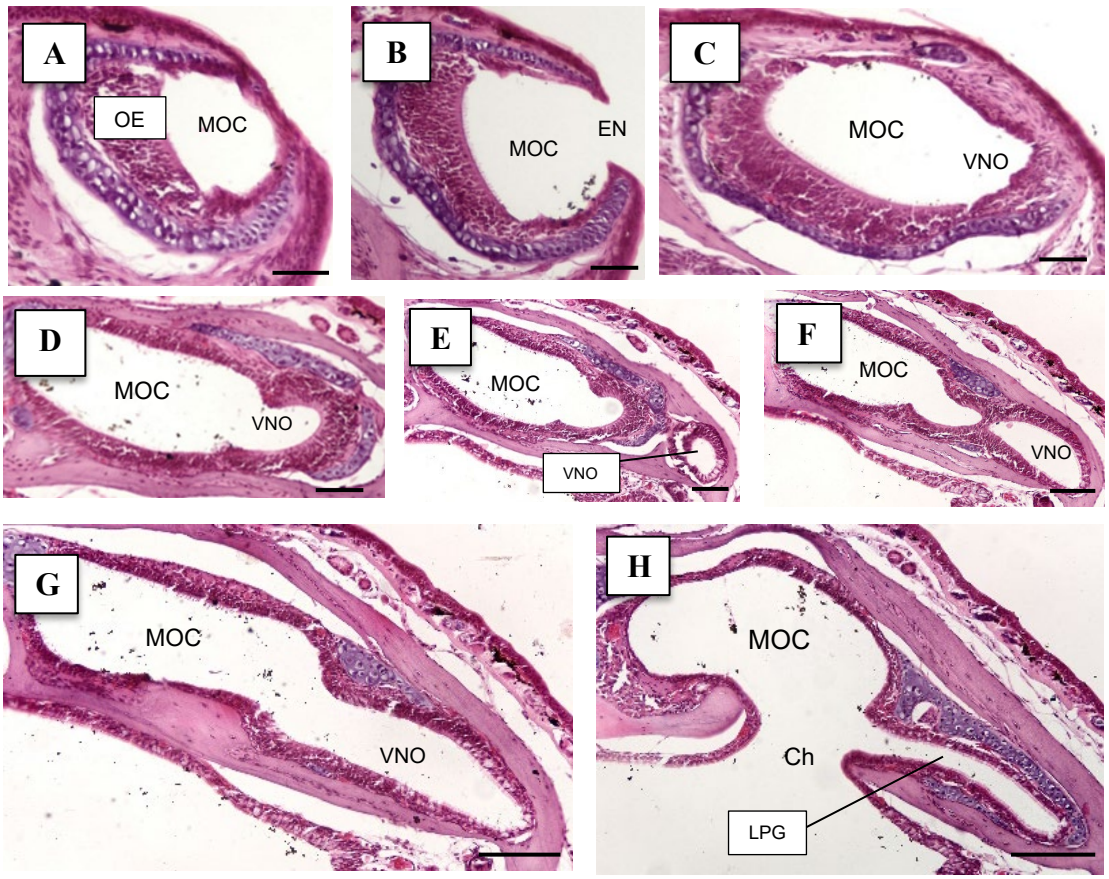

Figure 7. *Light micrographs of transverse sections through the adult* Desmognathus ocoee *olfactory organ.* ***A:*** *The main olfactory cavity (MOC) and the thick olfactory epithelium (OE).* ***B:*** *External nares (EN) and the MOC.* ***C:*** *The wider MOC and the vomeronasal organ (VNO).* ***D, E, F, G:*** *Both the MOC and VNO appear narrow and elongated. The epithelium appears thinner compared to the rostral region.* ***H:*** *Very back of the nose: The MOC at the level of the choana (Ch) and the lateral palatal groove (LPG). Scale bar (A, B, C): 100 µm. Scale bar (D, E, F, G, H): 200 µm.*

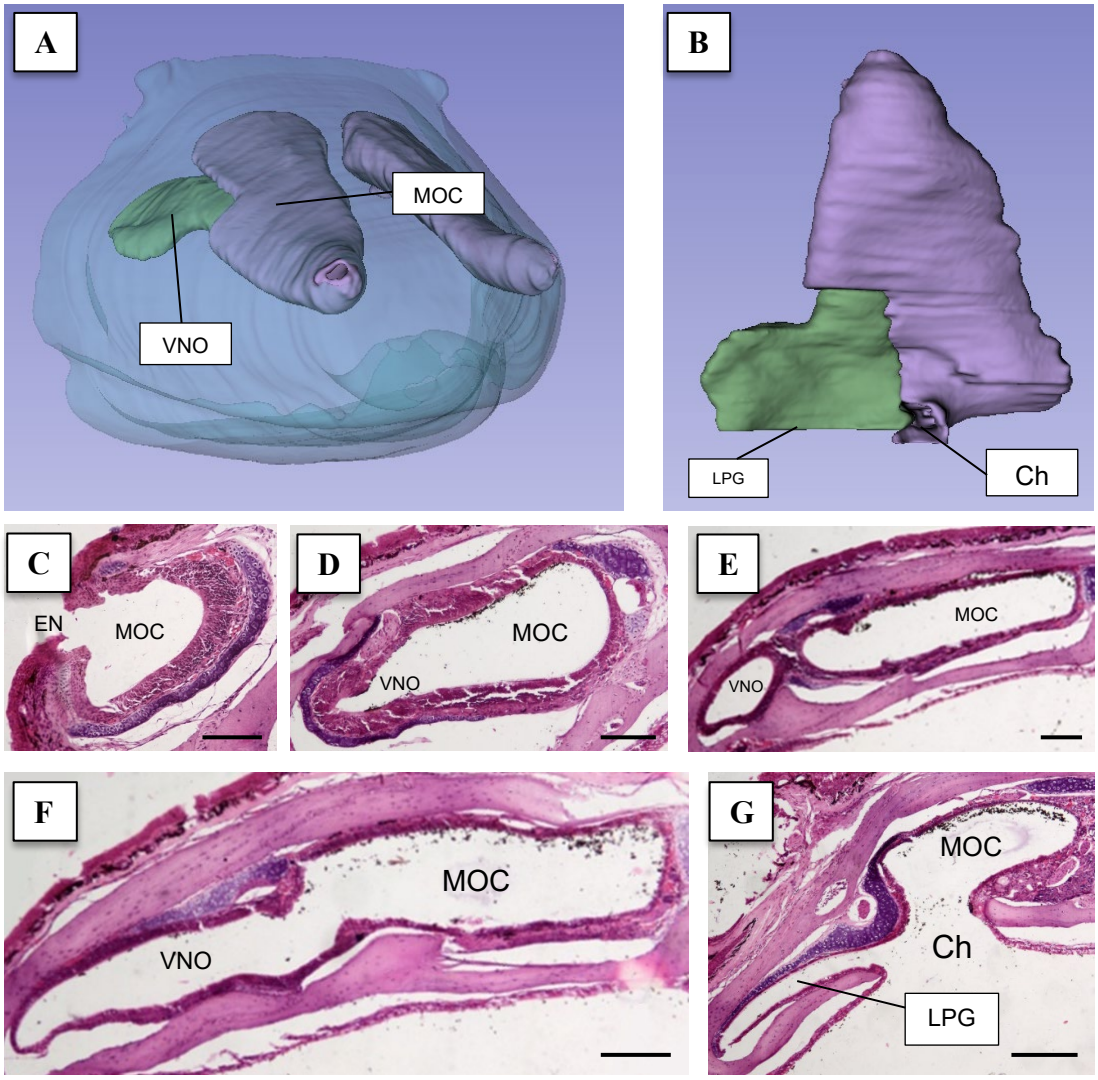

Figure 8. *Tridimensional reconstruction and light micrographs of transverse sections through the adult* Desmognathus amphileucus *olfactory organ.* ***A:*** *Anterolateral view of the 3D reconstruction of both olfactory organs. MOC is shown in purple, VNO is in light green.* ***B:*** *Ventral view of the 3D reconstruction of both olfactory organs. MOC is shown in purple, VNO is in light green.* ***C:*** *External nares (EN) and the MOC.* ***D:*** *The main olfactory cavity (MOC) is wider, while the vomeronasal organ (VNO) appears ventrolaterally.* ***E, F:*** *Further posteriorly, both the MOC and VNO are more dorso-ventrally compressed.* ***G:*** *MOC and VNO at the level of the choana (Ch), at the very back of the nose. Scale bar (C, D): 100 µm. Scale bar (E, F, G): 400 µm.*

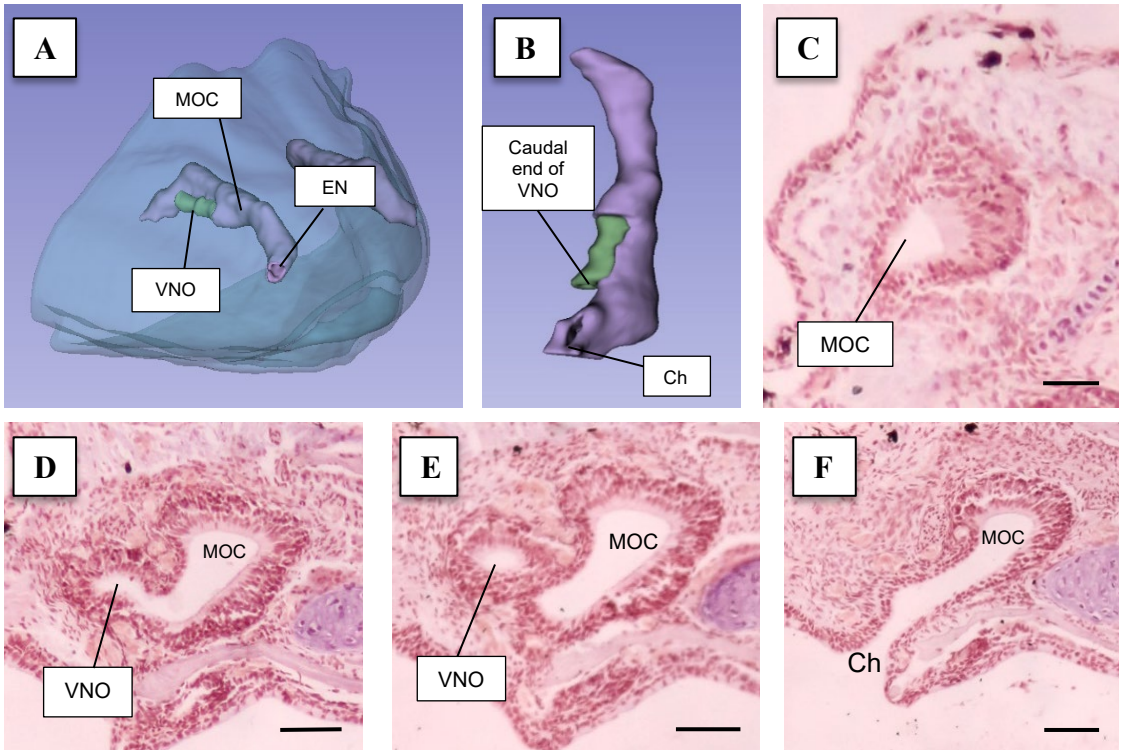

Figure 9. *Tridimensional reconstruction and light micrographs of transverse sections through the larval olfactory organ of* Desmognathus aureatus*.* ***A:*** *Anterolateral view of the 3D reconstruction of both olfactory cavities. MOC is shown in purple, VNO is in dark green.* ***B:*** *Ventral view of the 3D reconstruction of both the olfactory organs.* ***C:*** *Main olfactory cavity* ***(****MOC) posterior to the external nares.* ***D, E:*** *The MOC and the vomeronasal organ (VNO).* ***F:*** *Posterior end of the nose and choana (Ch). Scale bar: 50 µm.*

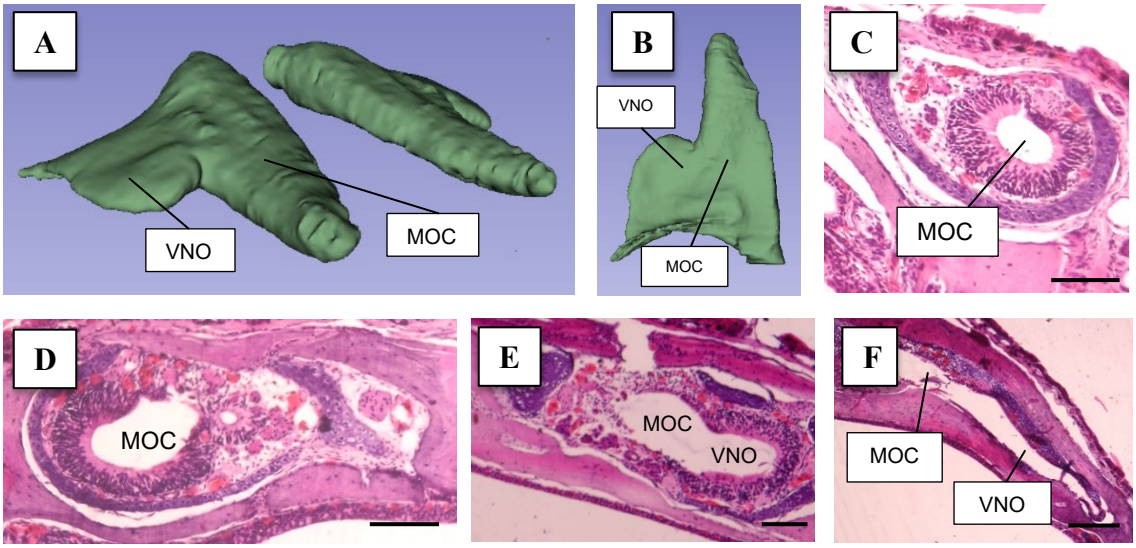

Figure 10. *Tridimensional reconstructions and light micrographs of transverse sections through the adult* Desmognathus aureatus *olfactory organ. Note: the boundary between the MOC and the VNO was not apparent and thus both organs are shown in green.* ***A:*** *Anterolateral view of the 3D reconstruction of the olfactory cavity.* ***B:*** *Ventral view of the 3D reconstruction of both olfactory organs.* ***C:*** *The main olfactory cavity (MOC).* ***D, E:*** *The MOC and the vomeronasal organ (VNO).* ***F:*** *Posterior end of the nose, with very dorso-ventrally compressed MOC and VNO. Scale bar (C, D, E): 200 µm. Scale bar (F): 400 µm.*

Expression Patterns of Olfactory-related Genes in Direct-Developing Plethodontids

In situ hybridization with the $G\alpha_{olf}$ anti-sense probe in direct-developing, terrestrial species revealed that the mRNA expression was restricted to the MOC of *E. eschscholtzii* adults (Fig. 11A-C) and *P. shermani* juveniles (Fig. 12A-D) except for the most lateral part of the MOC (in Fig. 12A, the faint coloration in the VNO represents background, non-specific expression). In *D. wrighti* adults, $G\alpha_{olf}$ was expressed in the

MOC, but also in the most medial part of the VNO (Fig. 13A-C). No detectable expression of $G\alpha_{i2}$ mRNA was observed in these species.

The mRNA expression of the G protein $G\alpha_o$ was more variable across taxa. In all species it is expressed in the more rostral regions of both the MOC and the VNO, but further posteriorly in the nose, its expression appeared to be restricted to the VNO in *E. eschscholtzii* adults (Fig. 11G, H), while in *P. shermani* juveniles, it was found expressed in the whole cavity, though the expression was generally more intense in the VNO (Fig. 12E). Expression of the *trpc2* ion channel was exclusively in the VNO. However, *trpc2* expression was concentrated in the lateral part of the VNO of *E. eschscholtzii* adults (Fig. 11D, E) but in the most medial part of the VNO of *D. wrighti* adults (Fig 13D).

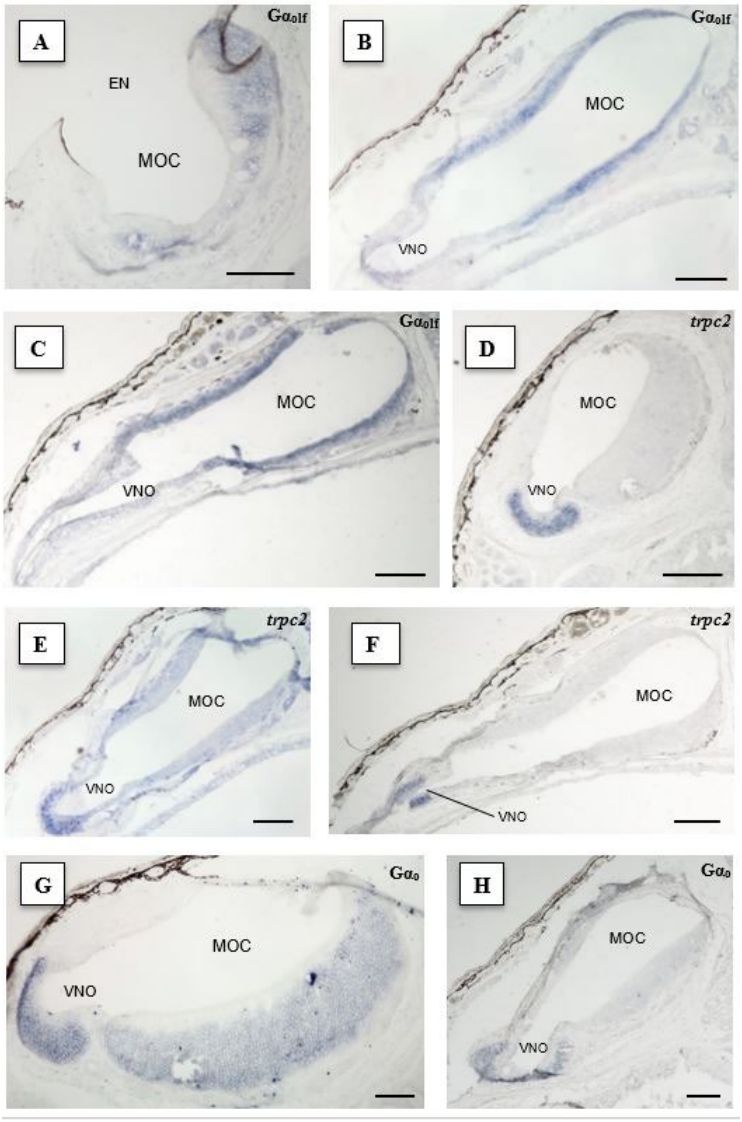

Figure 11. *Representative photomicrographs of chemosensory epithelia from* Ensatina eschscholtzii *adults showing mRNA expression of* $G\alpha_{olf}$ *and trpc2.* ***A:*** *Anterior olfactory cavity showing* $G\alpha_{olf}$ *mRNA expression in the most medial part of the MOC (medial to right in figure).* ***B:*** *Middle olfactory cavity showing* $G\alpha_{olf}$ *mRNA expression in most parts of the MOC.* ***C:*** *Caudal olfactory cavity, showing* $G\alpha_{olf}$ *mRNA expression in the MOC.* ***D:*** *Anterior olfactory cavity showing trpc2 mRNA expression in the VNO.* ***E:*** *Middle olfactory cavity showing trpc2 mRNA expression in the VNO.* ***F:*** *Caudal olfactory cavity showing trpc2 mRNA expression in the most lateral part of the VNO.* ***G:*** *Anterior olfactory cavity showing* $G\alpha_o$ *mRNA expression in both the MOC and the VNO.* ***H:*** *Middle level of olfactory cavity showing* $G\alpha_o$ *mRNA expression exclusively in the VNO. Scale bar (A, H): 200 µm; scale bar (B, C, D, E, F, G): 300 µm.*

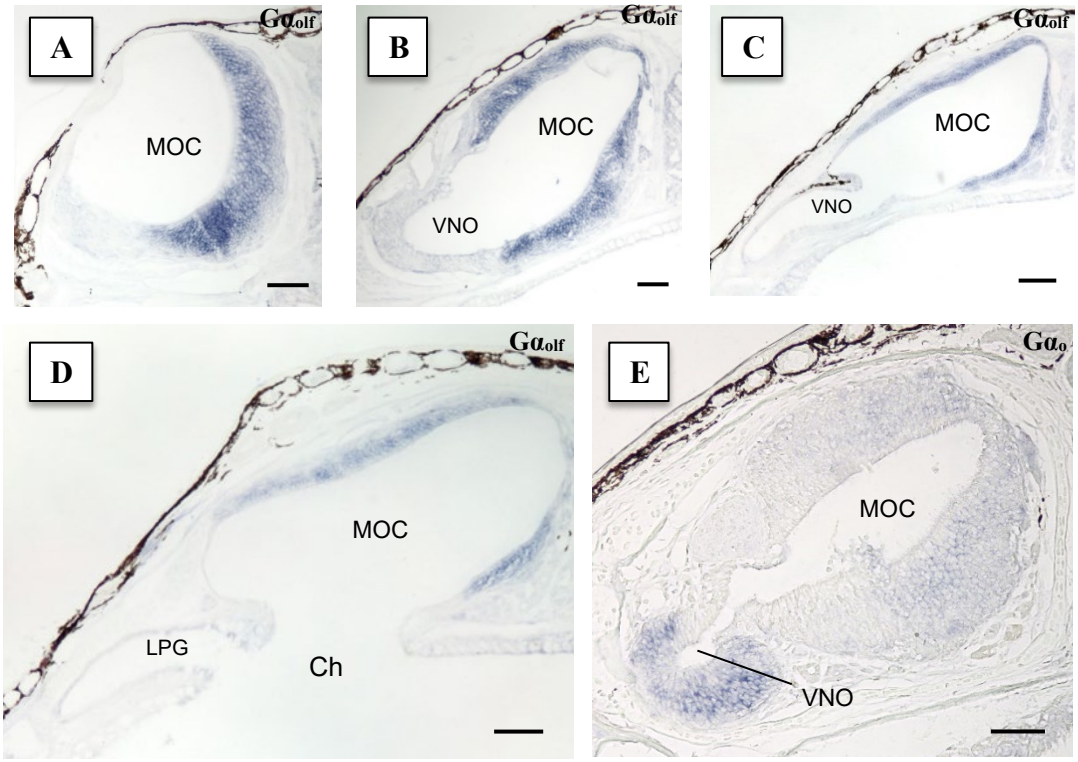

Figure 12. *Representative photomicrographs of chemosensory epithelia from* Plethodon shermani *juveniles showing* $G\alpha_{olf}$ *and* $G\alpha_{o}$ *mRNA expression.* ***A:*** *Anterior olfactory cavity showing* $G\alpha_{olf}$ *mRNA expression in most rostral region of the MOC.* ***B:*** *Middle level of olfactory cavity showing* $G\alpha_{olf}$ *mRNA expression in the MOC.* ***C:*** *Caudal olfactory cavity showing* $G\alpha_{olf}$ *mRNA expression in most parts of the MOC.* ***D:*** *Back of the olfactory cavity showing* $G\alpha_{olf}$ *mRNA expression in most parts of the MOC.* ***E:*** *Middle level of olfactory cavity showing* $G\alpha_{o}$ *mRNA expression in the VNO and less intensively in the MOC. Scale bar (A, B, E): 100 µm. Scale bar (C, D): 150 µm.*

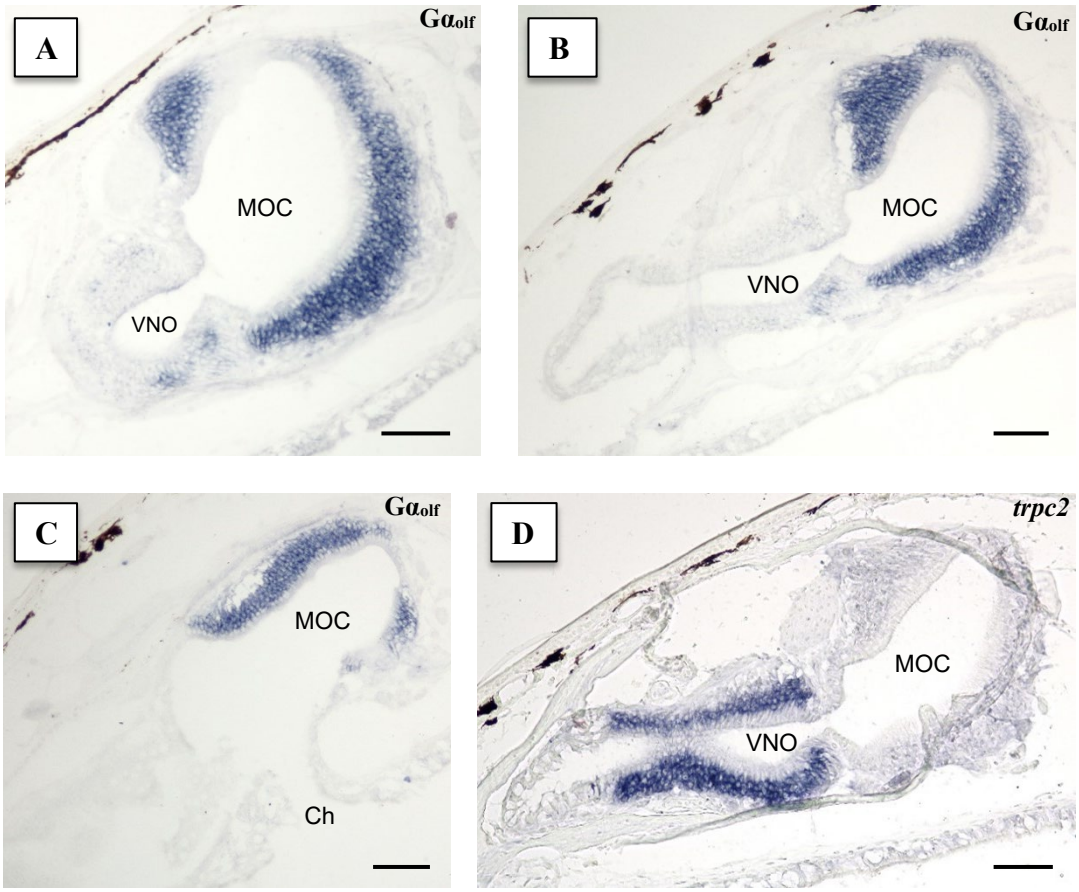

Figure 13. *Representative photomicrographs of chemosensory epithelia from* Desmognathus wrighti *adults showing mRNA expression of* $G\alpha_{olf}$ *and trpc2.* ***A:*** *Olfactory cavity showing* $G\alpha_{olf}$ *mRNA expression in most of the MOC and part of the VNO.* ***B:*** *Caudal olfactory cavity showing* $G\alpha_{olf}$ *mRNA expression in the whole MOC.* ***C:*** *Very back of the olfactory cavity showing* $G\alpha_{olf}$ *mRNA expression in the roof and most medial part of the MOC.* ***D:*** *Caudal olfactory cavity showing trpc2 mRNA expression in the most medial part of the VNO. Scale bar: 100 µm.*

Expression Pattern of Olfactory Components in Biphasic Plethodontids

In adult *D. ocoee*, $G\alpha_{olf}$ was expressed from the very anterior region of the MOC all the way to the posterior end. As the olfactory cavity enlarged caudally, the

mRNA was also expressed in the most medial part of the VNO (Fig. 14A, B, C). In *D. amphileucus* larvae, $G\alpha_{olf}$ was expressed in the whole MOC (Fig. 15A), while in *D. amphileucus* adults, it was expressed in both the MOC and in the VNO, although fewer cells in the most posterior region of the cavity expressed the mRNA (Fig. 16A). In *D. aureatus* larvae, the mRNA was expressed in the MOC (Fig. 17D), while in *D. aureatus* adults, it was expressed in the medial dorsal and ventral MOC (Fig. 17A). As with the direct-developing species, I did not detect expression of $G\alpha_{i2}$ RNA in any of my biphasic species.

The $G\alpha_o$ mRNA was expressed in *D. ocoee* adults both in the most medial part of the MOC and the whole VNO and, more caudally, it was expressed in almost the whole MOC (more intensely in the most lateral part of it) and just in the medial part of the VNO (Fig. 14G, H). In *D. amphileucus* larvae, $G\alpha_o$ was expressed in the whole cavity (Fig. 15D). In *D. amphileucus* adults, $G\alpha_o$ was found expressed in the whole MOC and VNO, but only in the medial VNO further posteriorly in the cavity (Fig. 16D, E, F).

Expression of the *trpc2* ion channel in *D. ocoee* adults was observed in the whole rostral VNO and, more caudally, in just the most medial and medial parts of the VNO (Fig. 14D, E, F). In *D. amphileucus* larvae, it was mainly found in the VNO, but a few cells expressed that mRNA in the medial part of the MOC (Fig. 15B, C). In *D. amphileucus* adults, *trpc2* is expressed in the MOC rostrally, and in the whole cavity more caudally (Fig. 16B, C). In *D. aureatus* adults, *trpc2* is expressed in both the MOC and VNO (Fig. 17B, C). These were the only two species in which I detected *trpc2* expression in the MOC.

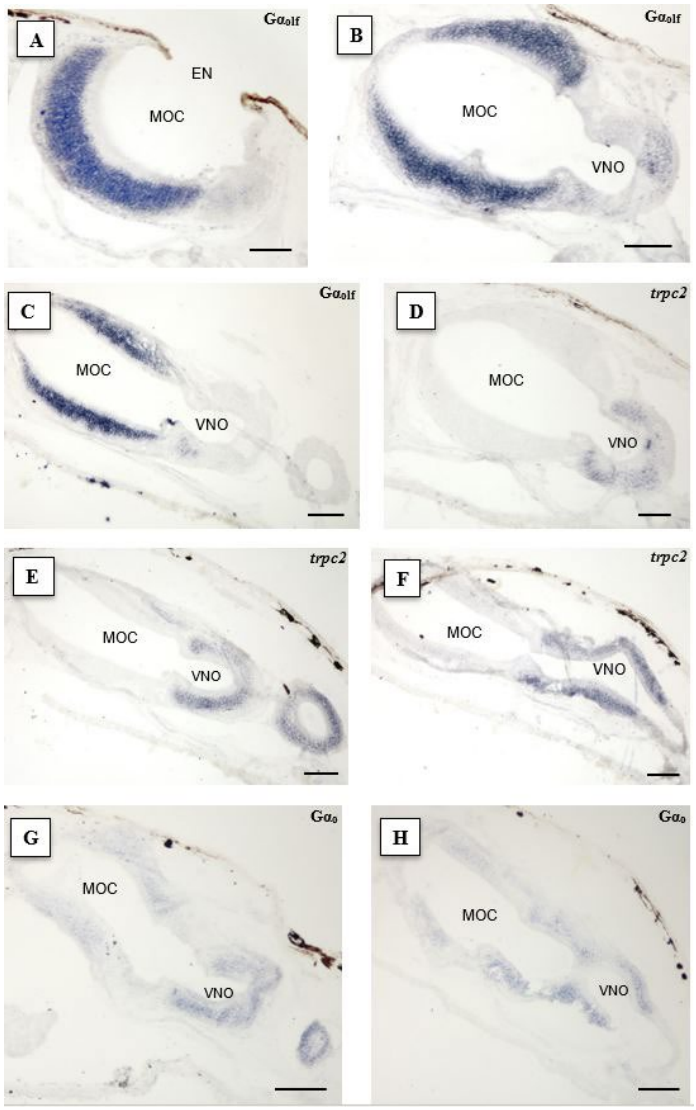

Figure 14. *Representative photomicrographs of chemosensory epithelia from* Desmognathus ocoee *adult showing mRNA expression of $G\alpha_{olf}$, trpc2 and $G\alpha_{o}$.* ***A:*** *Olfactory cavity showing expression of $G\alpha_{olf}$ in almost the whole MOC.* ***B:*** *Central part of the olfactory cavity showing expression of $G\alpha_{olf}$ in the MOC and, less intensely, in the VNO.* ***C:*** *Expression of $G\alpha_{olf}$ in the MOC and just the most medial part of the VNO.* ***D:*** *anterior part of the cavity shoving expression of trpc2 just in the VNO.* ***E:*** *Expression of trpc2 in the whole VNO.* ***F:*** *Middle olfactory cavity showing expression of trpc2 just in the medial and central part of the VNO, but not in the lateral part.* ***G:*** *Middle olfactory cavity showing expression of $G\alpha_{o}$ mRNA in the most medial part of the MOC and in the whole VNO.* ***H:*** *Caudal olfactory cavity showing expression of $G\alpha_{o}$ mRNA in almost the whole MOC and just the medial part of the VNO. Scale bar: 100 µm.*

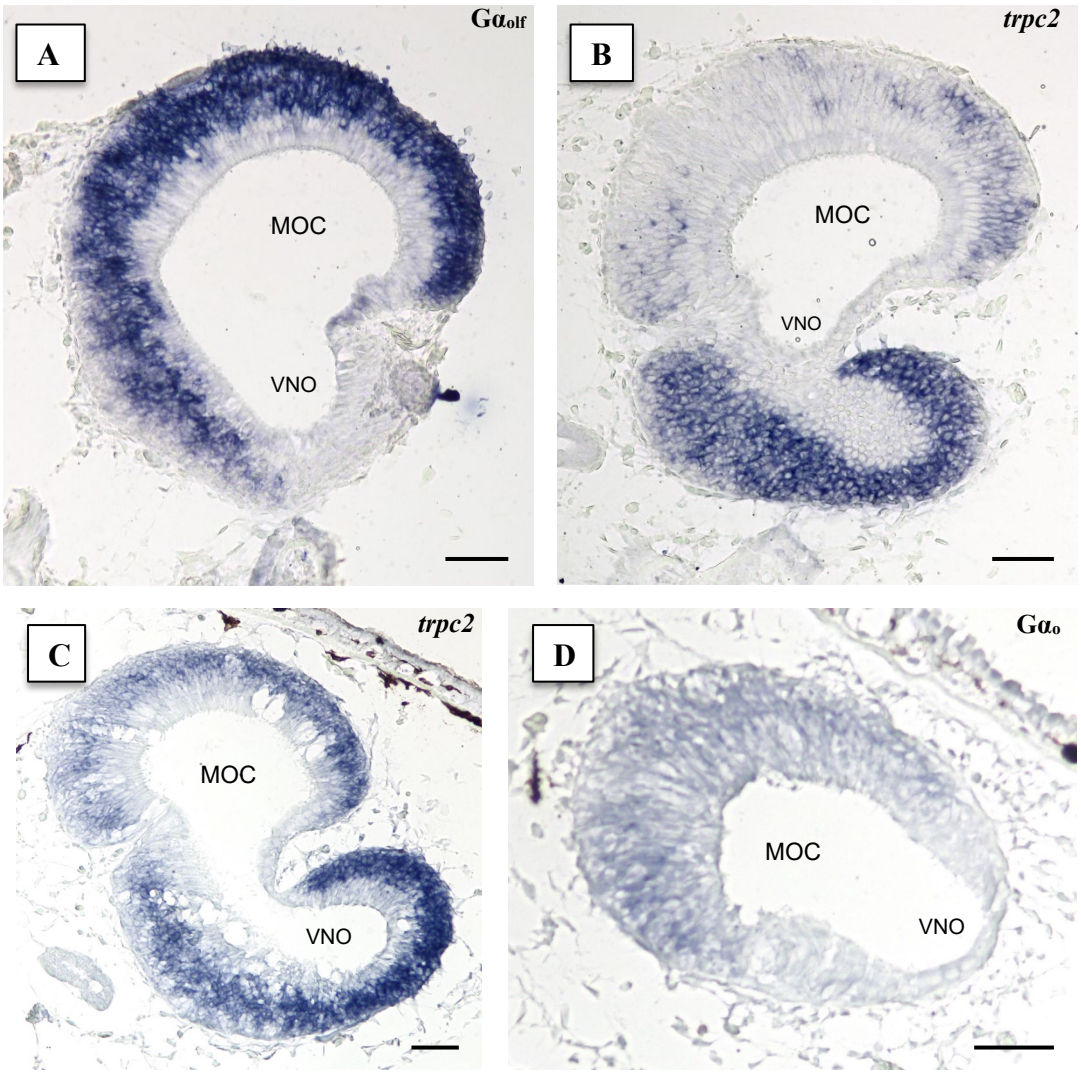

Figure 15. *Representative photomicrographs of chemosensory epithelia from larval* Desmognathus amphileucus *showing mRNA expression of* $G\alpha_{olf}$ *and trpc2.* ***A:*** *Olfactory cavity showing* $G\alpha_{olf}$ *mRNA expression in the whole MOC.* ***B:*** *Olfactory cavity showing trpc2 mRNA expression in part of the VNO and part of the dorsal MOC.* ***C:*** *Olfactory cavity showing trpc2* expression *in the whole cavity.* ***D:*** *Olfactory cavity showing* $G\alpha_o$ *expression. Scale bar: 100 µm.*

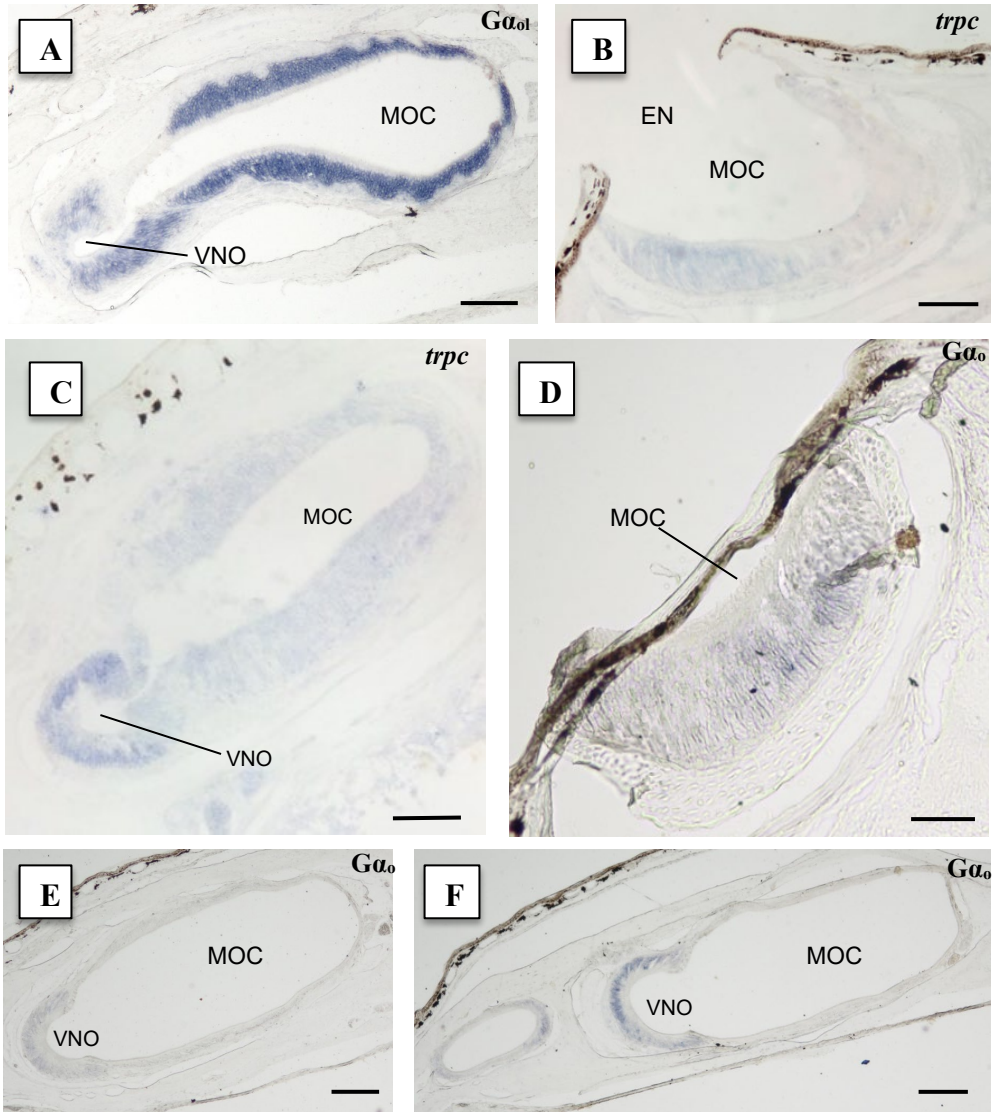

Figure 16. *Representative photomicrographs of chemosensory epithelia from* Desmognathus amphileucus *adults showing* $G\alpha_{olf}$ *and trpc2 mRNA expression.* ***A:*** *Olfactory cavity showing* $G\alpha_{olf}$ *mRNA expression in both the MOC and in the VNO.* ***B:*** *Anterior olfactory cavity showing trpc2 mRNA expression in the VNO* ***C:*** *Middle olfactory cavity showing trpc2 expression in the whole VNO and part of the MOC.* ***D:*** *Anterior olfactory cavity showing* $G\alpha_o$ *mRNA expression in the whole MOC.* ***E:*** *Middle olfactory cavity showing* $G\alpha_o$ *mRNA expression exclusively in the VNO.* ***F:*** *Posterior olfactory cavity showing* $G\alpha_o$ *mRNA expression in the most medial part of the VNO. Scale bar (A): 150 µm; scale bar (B, E, F, G): 200 µm; scale bar (C): 300 µm; scale bar (D): 100 µm.*

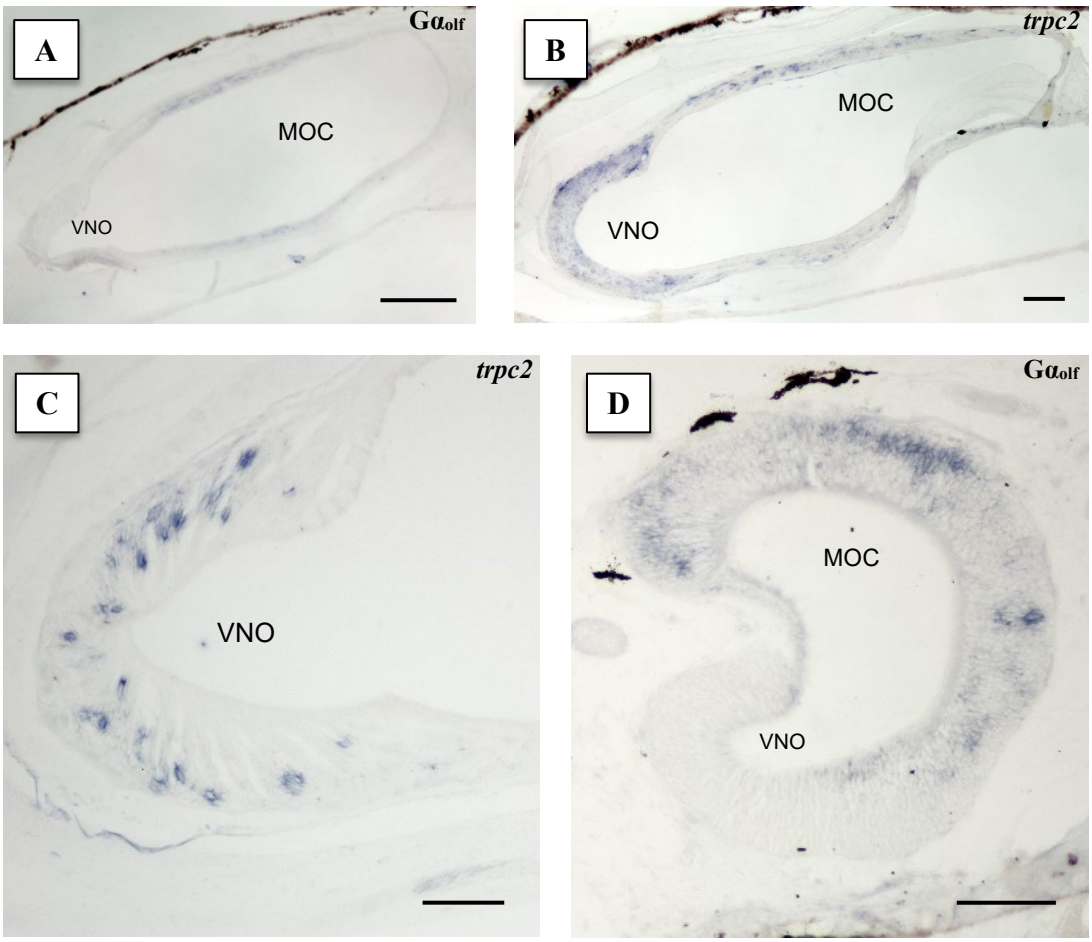

Figure 17. *Representative photomicrographs of chemosensory epithelia from* Desmognathus aureatus *adults and larvae showing* $G\alpha_{olf}$ *and trpc2 mRNA expression.* ***A:*** *Olfactory cavity of adult showing* $G\alpha_{olf}$ *mRNA expression in the central part of the MOC.* ***B:*** *Olfactory cavity of adult showing trpc2 mRNA expression in the VNO and, less intensely, in the MOC.* ***C:*** *VNO of adult showing trpc2 mRNA expression.* ***D:*** D. aureatus *larva olfactory cavity showing* $G\alpha_{olf}$ *mRNA expression in part of the MOC. Scale bar (A): 200 µm; scale bar (B, C, D): 100 µm.*

DISCUSSION

Comparative Morphology of the Plethodontid Nose

Size and shape of sensory organs can impact their function, and natural selection can optimize performance of such organs in particular environments and life histories (Dawley 2017). In this study, I investigated the histology and structure of the olfactory cavity in six species of plethodontids to test my prediction that life history and ecology may influence the morphology of the olfactory system. Because the structure of the plethodontid olfactory cavity has previously been investigated in several taxa, including species of *Plethodon*, *Desmognathus*, *Eurycea*, *Bolitoglossa*, *Aquiloeurycea*, *Chiropterotriton*, *Dendrotriton* and *Thorius* (Wilder 1913, 1925, Saint Girons and Zylberberg 1992a, b, Dawley 2017), I integrate my results with previous observations to describe broader patterns of sensory organ morphology across the Plethodontidae.

The results from my histology and 3D reconstructions largely supported my prediction that animals with similar ecologies (terrestrial vs. aquatic) would have similar nasal cavity morphologies. Terrestrial, direct-developing species in the genus *Plethodon*, for example, have similar cavity shapes and epithelial thicknesses, based on my observations of *P. shermani* (adults and juveniles – my study), and *P. cinereus* (adults) and *P. glutinosus* (adults) (Dawley 2017). In addition, I noticed that comparison of juvenile and adult life stages of *P. shermani* showed no substantial differences; they both have the same organ shape and the same relative olfactory epithelium thickness

throughout the whole cavity, showing that there are no drastic changes in the olfactory organ throughout the animal's development after hatching (this pattern was also noted by Dawley 2017). Adult *Ensatina eschscholtzii*, another terrestrial direct developer, were quite similar to *Plethodon* species in olfactory organ morphology.

Similarities in morphology were also apparent when comparing the closely related, direct-developing *D. wrighti* and *D. organi* (studied by Dawley 2017). Both *D. wrighti* and *D. organi* are terrestrial species but are much smaller bodied than the *Plethodon* and *Ensatina* I examined. *Desmognathus organi* possesses laterally directed external nares and nasal organs that are more vertically oriented than those of *Plethodon* species (characterized by Dawley 2017); I noted a similar situation for *D. wrighti.*

I did observe a few differences across terrestrial species, but these differences were relatively minor. The general shape of the MOC in *P. glutinosus* is wider than that of *P. cinereus*, and it has an overall thinner olfactory epithelium (Dawley 2017). At the level of the external nares, the MOC epithelium of *P. shermani* adults seemed to be relatively thinner than that of both *P. cinereus* and *P. glutinosus* adults. Furthermore, midway through the nose, the VNO in *P. shermani* adults was relatively wider compared to that of both *P. glutinosus* and *P. cinereus* adults.

As in the terrestrial direct developers, many aspects of the morphology of the olfactory cavity in adults of biphasic *Desmognathus* species are likewise similar in species with similar habitat preferences. *Desmognathus ochrophaeus* and its close relative *D. ocoee* are moderately small salamanders that prefer a more aquatic 'streamside' habitat than *D. wright* or *D. organi* (Dawley 2017). The head of *D.*

ochrophaeus appears flattened dorso-ventrally, as in most other *Desmognathus* species, and its snout is narrow and rounded (Sherman 1941). Streamside *D. ocoee* has a very similar head shape. As in most other desmognathines, the entire nasal chamber is dorso-ventrally compressed and horizontally oriented in *D. ochrophaeus* (Dawley 2017). The external nares in *D. ochrophaeus* are lateral rather than dorsal as in *D. amphileucus* (a more aquatic species). I found that *D. ocoee* shared all these features.

The aquatic/semiaquatic *Desmognathus* species also possess numerous morphological similarities. They have remarkably dorso-ventrally flattened heads as adults, as part of their feeding and burrowing adaptations (Schwenk and Wake 1993), and the shape of their heads might explain the laterally extended and dorso-ventrally compressed nasal chambers in these taxa (Dawley 2017). Specifically, I found that the olfactory organ of semiaquatic *D. amphileucus* was very like that previously described in *D. quadramaculatus* (Dawley 2017), which may have been the same species or not depending on the source of Dawley's specimen (Pyron and Beamer 2022). In particular, the external nares of both species are somewhat dorsal, and the nasal cavity is quite dorso-ventrally compressed and horizontally oriented.

Desmognathus aureatus is completely aquatic, and smaller than *D. amphileucus* (Martof 1962). The two species often co-occur. The aquatic larvae of *D. aureatus* possess a tubular organ with a thick olfactory epithelium, and this thickness is maintained throughout the whole length of the nose. In addition, the external nares are situated laterally. *Desmognathus aureatus* adults, in contrast with larvae, have dorsally situated external nares. The main olfactory epithelium is notably thin and flat throughout, and it

remains like that even while the vomeronasal epithelium expands. Dawley (2017) previously described this feature of *D. aureatus* (treated as *D. marmoratus*), which contrasts with all other plethodontid adults we both examined. The vomeronasal organ of *D. aureatus* is significantly widened, occupying more of the head than in *D. amphileucus*; the floor of the lateral diverticulum is also interrupted by the internal naris, while in other species, the internal naris occurs in the floor of the main olfactory cavity. *Desmognathus aureatus* also possesses unique internal nares, previously described by Martof (1962). They are like slit-like openings hidden in a fold on the roof of the mouth, in contrast with the internal nares of *D. amphileucus*, which are prominent and rounded openings in a more medial position.

A final pattern in morphology that I noticed across all species was a correlation between body size and thickness of the olfactory epithelium that was previously noted by Dawley (2017): the main olfactory epithelium in *D. wrighti* (my smallest focal species) appeared to be relatively thicker than that of *E. eschscholtzii* adults and *P. shermani* adults (larger focal species). It may be that a smaller bodied animal needs a similar number of sensory cells as a larger bodied animal, but must pack them into a smaller available space, resulting in a thicker olfactory epithelium (Dawley 2017). I did not, however, see a usually thick epithelium in *P. shermani* juveniles; this may be because the adult stage is when heightened olfactory function is most needed.

Comparative mRNA expression of G proteins and *trpc2* in the Plethodontid Nose

I predicted that the expression patterns of my selected olfactory components would be conserved in life stages with similar ecologies (e.g., in aquatic larvae and aquatic adults because they do not change habitat throughout their life), but that expression would be different in the larval stages versus adult stages of my biphasic species with terrestrial adults (related to the change in habitat between these two life stages). Of the four olfactory components selected for examination, in situ hybridization revealed the mRNA expression patterns of three ($G\alpha_{olf}$, $G\alpha_{o}$ and *trpc2*) in the sensory epithelium of the olfactory organ of my six plethodontid species (Table 4). Although the same protocol was used to investigate mRNA expression of $G\alpha_{i2}$, there was no mRNA expression detected. Preliminary transcriptome analysis of mRNA found in the *P. shermani* nasal epithelium also found much lower levels of transcription of $G\alpha_{i2}$ relative to the other two (Wilburn, D.B., pers. comm.). Moreover, previous efforts to isolate V1R genes (the GPCR family associated with $G\alpha_{i2}$) from *P. shermani* were not successful (Kiemnec-Tyburczy et al. 2012). These observations lead me to conclude that neither $G\alpha_{i2}$ nor V1Rs are highly expressed in the VNO or MOE of plethodontids; the lack of $G\alpha_{i2}$ staining on sections is likely to represent extremely low levels of expression, rather than an issue with the experimental technique.

Table 4. *mRNA expression of Gαolf, trpc2 and Gαo in the MOC and the VNO of the species examined in this study. The X's indicate no expression was observed on sections, while 'Not Tested' indicates that no in situ hybridization was performed. Results on adult* P. shermani *(from Kiemnec-Tyburczy et al. 2012) are also included in this table.*

Species name	Ecology	Region	$G\alpha_{olf}$	*trpc2*	$G\alpha_{o}$
E. eschscholtzii **adult**	**Terrestrial**	**MOC**	✓	✗	✓
E. eschscholtzii **adult**	**Terrestrial**	**VNO**	✗	✓	✓
P. shermani **juvenile**	**Terrestrial**	**MOC**	✓	**Not tested**	✓
P. shermani **juvenile**	**Terrestrial**	**VNO**	✗	**Not tested**	✓
P. shermani **adult**	**Terrestrial**	**MOC**	✓	✗	✗
P. shermani **adult**	**Terrestrial**	**VNO**	✓	✓	✓
D. wrighti **adult**	**Terrestrial**	**MOC**	✓	✗	**Not tested**
D. wrighti **adult**	**Terrestrial**	**VNO**	✓ (most medial part)	✓ (medial part)	**Not tested**
D. ocoee **adult**	**Streamside**	**MOC**	✓	✗	✓
D. ocoee **adult**	**Streamside**	**VNO**	✓ (most medial part)	✓	✓
D. amphileucus **larva**	**Aquatic**	**MOC**	✓	✓ (part)	✓
D. amphileucus **larva**	**Aquatic**	**VNO**	✗	✓	✓
D. amphileucus **adult**	**Semiaquatic**	**MOC**	✓	✓ (part)	✓ (part)
D. amphileucus **adult**	**Semiaquatic**	**VNO**	✓	✓	✓
D. aureatus **larva**	**Aquatic**	**MOC**	✓	**Not tested**	**Not tested**
D. aureatus **larva**	**Aquatic**	**VNO**	✗	**Not tested**	**Not tested**
D. aureatus **adult**	**Aquatic**	**MOC**	✓	✓	**Not tested**
D. aureatus **adult**	**Aquatic**	**VNO**	✗	✓	**Not tested**

The results lend partial support for the hypothesis that the expression pattern of olfactory-related genes to be conserved in life history stages with similar ecologies. In the case of $G\alpha_{olf}$, it is found expressed in the MOC of all three direct developing species,

except for the very lateral part of the MOC near the VNO. This is likely because the boundary between the MOC and VNO is composed of non-sensory epithelium. In adult *P. shermani*, previous work showed that $G\alpha_{olf}$ is expressed in the MOC as well as the whole VNO (Kiemnec-Tyburczy et al. 2012). This is discordant to what I found for *P. shermani* juveniles, in which the protein is expressed exclusively in the MOC (not the VNO). This pattern indicates that expression of ORs (the receptors associated with $G\alpha_{olf}$) is generally, but not exclusively, restricted to the MOC in direct developers, and that expression can vary between juvenile and adult stages. By contrast with expression patterns of $G\alpha_{olf}$, the adult stages of all three direct-developing plethodontid species express *TRPC2* exclusively in the VNO, though *D. wrighti* expresses the ion channel in just part of the VNO, excluding the most lateral part of it.

Overall, there were many similarities across the terrestrial plethodontids, but the pattern of $G\alpha_o$ expression that I observed in my direct developing species were discordant with my prediction. Studies performed on *P. shermani* adults showed that V2R receptors (associated with $G\alpha_o$) are exclusively expressed in the VNO (Kiemnec-Tyburczy et al. 2012). This is unlike what I have found in juveniles, where $G\alpha_o$ (the G protein associated with the V2R receptors in rodents [Fleischer et al. 2009]) is expressed in both the MOC and the VNO. This shows that the expression pattern of this ion channel can change as the animal reaches sexual maturity, just as I saw with $G\alpha_{olf}$.

I also hypothesized that expression of olfactory genes would vary between the larval stages versus adult stages of my biphasic species, based on the differences in the environment those life stages inhabit. The expression of some components, however, did

not strictly fit this prediction (Table 4). The G protein $G\alpha_{olf}$, for example, is expressed exclusively in the MOC of both larval *D. amphileucus* and *D. aureatus* but in the MOC *and* the VNO in aquatic *D. amphileucus* adults (but not in the VNO of aquatic *D. aureatus* adults). The pattern in the streamside *D. ocoee* adults was like that in *D. amphileucus* (expression in both the MOC and the most medial part of the VNO).

The expression patterns of $G\alpha_o$ were similarly complex. The protein is expressed in the whole cavity (both MOC and VNO) in adult *D. ocoee* and adult and larval *D. amphileucus*. The expression of V2Rs (the GPCR family that interacts with $G\alpha_o$) is restricted to the VNO in adult *P. shermani* (Kiemnec-Tyburczy et al. 2012). Therefore, V2R expression appears to be more widespread in the olfactory cavity of aquatic species, but limited to the VNO in terrestrial species, presumably because that is the region that receives soluble, waterborne odorants.

Among my biphasic species, *trpc2* is more highly expressed in the accessory region of the nose (VNO) in adults with a more aquatic lifestyle, but it is still expressed in the VNO in species that are terrestrial. In particular, *trpc2* was expressed exclusively in the VNO only in *D. ocoee* (Table 4), while in adults of the other two biphasic species, the ion channel is found expressed in the whole nasal cavity, though the expression is higher in the VNO than the MOC. The same pattern is seen in *D. amphileucus* larvae (unfortunately, I do not have comparable data for *D. aureatus* larvae). I can conclude that although gene expression patterns were variable, in general ORs and V2Rs are found expressed in most parts of the nasal cavity of adults of biphasic species, and therefore

both the MOC and VNO likely play an important role in the detection of airborne and waterborne odorants in these plethodontids.

Conservation and diversification in olfactory gene expression across vertebrates

There is deep conservation of the major GPCR gene families across the vertebrate lineages (Strotmann et al. 2011). All families are found expressed in the olfactory epithelium in fishes, while in tetrapods they are more localized, with some expressed in the VNO and some in the MOC, but how they have been partitioned in those organs varies across taxa (Table 5). The compartmentalization of the olfactory system into MOC and VNO in tetrapods is thought to be an adaptation to life in both aquatic and terrestrial environments (Freitag et al. 1995), based on the partitioning of gene expression originally observed in mammals. But gene expression profiles in the separate compartments of the nose in adult amphibians are in fact highly variable. For example, in terrestrial *B. japonicus* adults, both $G\alpha_{olf}$ and $G\alpha_{o}$ are expressed in the VNO (Hagino-Yamagishi and Nakazawa 2011). In secondarily aquatic *Xenopus*, only more recently derived V2Rs are expressed in the expressed in the VNO, while the principal cavity (the equivalent of the MOC that contains the air-smelling epithelium) expresses “ancient” V2Rs, V1Rs and ORs (Freitag et al. 1995; Date-Ito et al. 2008).

Table 5. *Localization of olfactory receptors, associated G proteins and the TRPC2 channel in tetrapods. Empty cells indicate lack of data for that species. ORs: olfactory receptors; TRPC2: transient receptor potential cation channel, subfamily C, member 2. V1Rs: vomeronasal type 1 receptors; V2Rs: vomeronasal type 2 receptors.*

	MOC	**MOC**	**VNO**	**VNO**	**References**
	G proteins	**Receptors and TRPC2**	**G proteins**	**Receptors and TRPC2**	
Mus musculus **(Mammal)**	$G\alpha_{olf}$ (adult)	ORs (adult)	$G\alpha_{o}$	V1Rs, V2Rs (adult)	Liman & Dulac 2007; Fleischer et al. 2009
Xenopus laevis **(Anuran)**	$G\alpha_{olf}$, $G\alpha_{o}$ (adults)	V2Rs, TRPC2 (larva); ORs, V1Rs, V2Rs, ORs (adult)	$G\alpha_{o}$ (adults)	V2Rs, TRPC2 (larva); V2Rs (adult)	Freitag et al. 1995; Date-Ito et al. 2008; Sansone et al. 2014; Mezler et al. 2001
Rhinella arenarum **(Anuran)**	$G\alpha_{o,}$ $G\alpha_{olf}$ (larva)	V2Rs (larva)	$G\alpha_{o}$ (larva)	V2Rs (larva)	Jungblut et al. 2009
Hypsiboas pulchellus **(Anuran)**	$G\alpha_{o}$ (larva)	V2Rs (larva)	$G\alpha_{o}$ (larva)	V2Rs (larva)	Jungblut et al. 2009
Bufo japonicus **(Anuran)**			$G\alpha_{olf}$, $G\alpha_{o}$ (adult)		Hagino-Yamagishi & Nakazawa 2011
Cynops pyrrhogaster **(Caudate)**	$G\alpha_{o}$, $G\alpha_{olf}$, $G\alpha_{i2}$ (adult)		$G\alpha_{o}$, $G\alpha_{olf}$ (adult)		Nakada et al. 2014
Ichthyosaura alpestris **(Caudate)**	$G\alpha_{o}$ (adult)				Różański et al. 2020
Ambystoma tigrinum **(Caudate)**		ORs (adult)		ORs (adult)	Marchand et al. 2004
Plethodon shermani **(Caudate)**	$G\alpha_{olf}$ (adult)		$G\alpha_{olf}$ (adult)	V2Rs, TRPC2 (adult)	Kiemnec-Tyburczy et al. 2012

As for salamanders (caudate amphibians), the expression of olfactory receptors and related genes had only been characterized in the adults of four species before I began my study: *Cynops pyrrhogaster* (Nakada et al. 2014), *Ambystoma tigrinum* (Marchand et

al. 2004), *Plethodon shermani* (Kiemnec-Tyburczy et al. 2012), and *Ichthyosaura alpestris* (Różański et al. 2020). In adult *C. pyrrhogaster*, an almost entirely aquatic newt, $G\alpha_o$ and $G\alpha_{olf}$ are both expressed in the MOC and in the VNO, though with many fewer $G\alpha_{olf}$ expressing receptor cells in the VNO (Nakada et al. 2014). Adult *P. shermani* expresses $G\alpha_{olf}$ in the MOC, and V2Rs, *TRPC2* and some limited $G\alpha_{olf}$ in the VNO (Kiemnec-Tyburczy et al. 2012). In adult *A. tigrinum*, ORs appear to be expressed both in the MOC and, less intensively, in the VNO (Marchand et al. 2004). In the terrestrial adult form of the alpine newt *I. alpestris* (which breeds in water but spends much of its life on land) the protein $G\alpha_o$ is found expressed exclusively in the MOC (Różański et al. 2020).

Patterns of gene expression likewise vary across anuran life stages; generally, sensory cells of the MOC and the VNO are not fully separated at the molecular level, as all major families of olfactory receptor genes (ORs, V1Rs, and V2Rs) have been observed to be expressed in the main olfactory epithelium during larval stages of various taxa (Hagino-Yamagishi et al. 2004; Date-Ito et al. 2008, Jungblut et al. 2009). Larval anurans generally express $G\alpha_o$ (and presumably V2Rs) and $G\alpha_{olf}$ in the MOC and $G\alpha_o$ in the VNO (Table 5 and references therein). And *trpc2* is (unsurprisingly) found expressed in both the main olfactory epithelium and the VNO in *X. laevis* tadpoles (Sansone et al. 2014). Interestingly, the larval expression of ancient V2Rs in the principal cavity of *Xenopus* is mostly lost during metamorphosis as the olfactory epithelium of that cavity transforms into the “air nose”, and the newly formed middle cavity, or “water nose”, retains the ability to detect of waterborne odors by expressing V1Rs, ancient V2Rs, and ORs (Date-Ito et al. 2008, Syed et al. 2017).

Taking into consideration these amphibian taxa and comparing them to my study species, it is noteworthy that the protein $G\alpha_o$ (associated with V2Rs) is expressed in most parts of the nasal cavity of aquatic species, ranging from frogs to newts to salamanders, suggesting that these receptors are of major importance for smelling waterborne odorants. The strict partitioning of olfactory components first documented in mammals is not observed in amphibians. There are numerous cases in which the expression of *trpc2* and $G\alpha_o$ overlaps in the nasal cavity of my study species, especially in biphasic ones. Since *trpc2* is correlated with the site of detection of pheromones in mammals (Venkatachalam and Montell 2007), and it is found in the whole cavity of the most strictly aquatic species, *D. amphileucus* and *D. aureatus*, this supports the hypothesis that these species use their whole cavity to sense waterborne odorants that may act as pheromones.

The present study has informed our understanding of the variation in receptor expression, but my research had some limitations that warrant consideration and present opportunities for future study. Due to constraints on how quickly I could process specimens, there was variation in the duration of time that animals spent in the laboratory environment before they were euthanized (see Appendix A for more details). Although none of my specimens underwent metamorphosis while in captivity, the animals were housed in individual boxes and fed invertebrates that are not native to their natural environment. Little is known about how the environment may shape the expression of GPCR families in neurons, but it is possible that the housing conditions could have affected gene expression in animals housed in captivity for longer periods of time. Unfortunately, most previous research on olfactory gene expression has been conducted

on captively bred animals (e.g., *X. laevis* [Sansone et al. 2014], *C. pyrrhogaster* [Nakada et al. 2014], *B. japonicus* [Hagino-Yamagishi & Nakazawa 2011]) and thus more research is needed to understand environmentally induced expression changes in the olfactory system. Ideally, future studies on natural populations would euthanize animals right after field collection to minimize the chance that expression changes are induced by housing in captivity.

This is the first study that has investigated multiple species within a monophyletic group of amphibians to understand how different life histories may influence the morphology of the olfactory organ, as well as patterns of olfactory gene expression. Although additional studies of some life stages within my taxa are warranted, the results show that there is both stasis and diversification in gene expression patterns and morphology within the extremely heterogeneous family of plethodontid salamanders, and that differences in life history and ecology can explain some, but not all, of this variation.

REFERENCES

Altig, R., and McDiarmid, R. (2015). Handbook of larval amphibians of the United States and Canada. Cornell University Press.

Arnold, S. J., Kiemnec-Tyburczy, K., and Houck, L. D. (2017). The evolution of courtship behavior in plethodontid salamanders, contrasting patterns of status and diversification. Herpetologica 73, 190-205.

Baxi, K. N., Dorries, K. M., and Eisthen, H. L. (2006) Is the vomeronasal system really specialized for detecting pheromones? Trends in Neurosciences 29, 1-7.

Beachy, C. K., Ryan, T. J., and Bonett, R. M. (2017). How metamorphosis is different in plethodontids: larval life history perspectives on life-cycle evolution. Herpetologica 73, 252-258.

Beamer, D. A., and Lamb, T. (2008). Dusky salamanders (*Desmognathus*, Plethodontidae) from the Coastal Plain: multiple independent lineages and their bearing on the molecular phylogeny of the genus. Molecular Phylogenetics and Evolution 47, 143-153.

Belluscio, L., Gold, G. H., Nemes, A., and Axel, R. (1998). Mice deficient in G(olf) are anosmic. Neuron 20, 69-81.

Benzekri, N. A., and Reiss, J. O. (2012). Olfactory metamorphosis in the coastal tailed frog *Ascaphus truei* (Amphibia, Anura, Leiopelmatidae). Journal of Morphology 273, 68-87.

Bruce, R. C. (1985). Larval period and metamorphosis in the salamander *Eurycea bislineata*. Herpetologica 41, 19-28.

Bruce, R. C. (1989). Life history of the salamander *Desmognathus monticola*, with a comparison of the larval periods of *D. monticola* and *D. ochrophaeus*. Herpetologica 45, 144-155.

Bruce, R. C. (2005). Theory of complex life cycles: application in plethodontid salamanders. Herpetological Monographs 19, 180-207.

Bruce, R. C. (2019). Life history evolution in plethodontid salamanders and the evolutionary ecology of direct development in dusky salamanders (*Desmognathus*). Herpetological Review 50, 673-682.

Buck, L., and Axel, R. (1991). A novel multigene family may encode odorant receptors: a molecular basis for odor recognition. Cell 65, 175-187.

Butler, K., Zorn, A. M., and Gurdon, J. B. (2001). Nonradioactive in situ hybridization to *Xenopus* tissue sections. Methods 3, 295-373.

Carroll, S. B., Grenier, J. K., and Weatherbee, S. D. (2001). From DNA to diversity: molecular genetics and the evolution of animal design. Blackwell Science.

Chippindale, P. T., Bonett, R. M., Baldwin, A. S., and Wiens, J. J. (2004). Phylogenetic evidence for a major reversal of life-history evolution in plethodontid salamanders. Evolution 58, 2809-2822.

Date-Ito, A., Ohara, H., Ichikawa, M., Mori, Y., and Hagino-Yamagishi, K. (2008). *Xenopus* V1R vomeronasal receptor family is expressed in the main olfactory system. Chemical Senses, 33, 339-346.

Dawley, E. M. (1992). Sexual dimorphism in a chemosensory system: the role of the vomeronasal organ in salamander reproductive behavior. Copeia 1992, 113-120.

Dawley, E. M. (1998). Species, sex, and seasonal differences in VNO size. Microscopy Research and Technique 41, 506-518.

Dawley, E. M. (2017). Comparative morphology of plethodontid olfactory and vomeronasal organs: how snouts are packed. Herpetological Monographs 31, 169-209.

Dawley, E. M., and Bass, A. H. (1989). Chemical access to the vomeronasal organs of a plethodontid salamander. Journal of Morphology 200, 163-174.

Duc, N. M., Kim, H. R., and Chung, K. Y. (2015). Structural mechanism of G protein activation by G protein-coupled receptor. European Journal of Pharmacology 763(Pt B), 214-22.

Duellman, W. E., and Trueb, L. (1994). Biology of amphibians. McGraw-Hill, New York.

Dulac, C., and Axel, R. (1995). A novel family of genes encoding putative pheromone receptors in mammals. Cell 83, 195-206.

Eisthen, H. L. (1992). Phylogeny of the vomeronasal system and of receptor cell types in the olfactory and vomeronasal epithelia of vertebrates. Microscopy Research and Technique 23, 1-21.

Eisthen, H.L. (1997). Evolution of vertebrate olfactory systems. Brain, Behavior and Evolution 50, 222-233.

Fleischer, J., Breer, H., and Strotmann, J. (2009). Mammalian olfactory receptors. Frontiers in Cellular Neuroscience 3, 787.

Forester, D. C. (1977). Comments on the female reproductive cycle and philopatry by *Desmognathus ochrophaeus* (Amphibia, Urodela, Plethodontidae). Journal of Herpetology 11, 311-316.

Freitag, J., Krieger, J., Strotmann, J., and Breer, H. (1995). Two classes of olfactory receptors in *Xenopus laevis*. Neuron 15, 1383-92.

Gaudin, A., and Gascuel, J. (2005). 3D atlas describing the ontogenic evolution of the primary olfactory projections in the olfactory bulb of *Xenopus laevis*. The Journal of Comparative Neurology 489, 403-424.

Gignac, P. M., Kley, N. J., Clarke, J. A., Colbert, M. W., Morhardt, A. C., Cerio, D., Cost, I. N., Cox, P. G., Daza, J. D., Early, C. M., Echols, M. S., Henkelman, M. R., Herdina, A. N., Holliday, C. M., Li, Z., Mahlow, K., Merchant, S., Muller, J., Orsbon, C. P., Paluh, D. J., Thies, M. L., Tsai, H. P., and Witmer, L. M. (2016). Diffusible iodine-based contrast-enhanced computed tomography (diceCT): an emerging tool for rapid, high-resolution, 3-D imaging of metazoan soft tissues. Journal of Anatomy 228, 889-909.

Hagino-Yamagishi, K., and Nakazawa, H. (2011). Involvement of Gαolf expressing neurons in the vomeronasal system of *Bufo japonicus*. Journal of Comparative Neurology, 519, 3189-3201.

Hagino-Yamagishi, K., Moriya, K., Kubo, H., Wakabayashi, Y., Isobe, N., Saito, S., Ichikawa, M., and Yazaki, K. (2004). Expression of vomeronasal receptor genes in *Xenopus laevis*. Journal of Comparative Neurology 472, 246-56.

Hairston, N. G. (1983). Growth, survival, and reproduction of *Plethodon jordani*: trade-offs between selective pressures. Copeia 1983, 1024-1035.

Herrada, G., and Dulac, C. (1997). A novel family of putative pheromone receptors in mammals with a topographically organized and sexually dimorphic distribution. Cell 90, 763-73.

Hilton, W. (1947). The hyobranchial skeleton of Plethodontidae. Herpetologica 3, 191-194.

Humason, G. L. (1979). Animal tissue techniques. W. H. Freeman.

Jones, K. S., and Weisrock, D. W. (2018). Genomic data reject the hypothesis of sympatric ecological speciation in a clade of *Desmognathus* salamanders. Evolution 72, 2378-2393.

Jungblut, L. D., Reiss, J. O., Paz, D. A., and Pozzi, A. G. (2009). Quantitative comparative analysis of the nasal chemosensory organs of anurans during larval development and metamorphosis highlights the relative importance of chemosensory subsystems in the group. Journal of Morphology 278, 1165-1308.

Jungblut, L. D., Paz, D. A., López-Costa, J. J., and Pozzi, A. G. (2009). Heterogeneous distribution of G protein alpha subunits in the main olfactory and vomeronasal systems of *Rhinella (Bufo) arenarum* tadpoles. Zoological Science 26, 722-728.

Jungblut, L. D., Reiss, J. O., and Pozzi, A. G. (2021). Olfactory subsystems in the peripheral olfactory organ of anuran amphibians. Cell and Tissue Research 383, 289-299.

Kerney, R., Gross, J., and Hanken, J. (2010). Early cranial patterning in the direct-developing frog *Eleutherodactylus coqui* revealed through gene expression. Evolution & Development 12, 373-382.

Kiemnec-Tyburczy, K. M., Woodley, S. K., Watts, R. A., Arnold, S. J., and Houck, L. D. (2012). Expression of vomeronasal receptors and related signaling molecules in the nasal cavity of a caudate amphibian (*Plethodon shermani*). Chemical Senses 37, 335-346.

Kiselyov, K., van Rossum, D. B., and Patterson, R. L. (2010). TRPC channels in pheromone sensing. Vitamins & Hormones 83, 197-213.

Lannoo, M. (2005). Amphibian declines: the conservation status of United States species. University of California Press.

Liberles, S. D., and Buck, L. B. (2006). A second class of chemosensory receptors in the olfactory epithelium. Nature 442, 645-650

Liman, E. R., and Innan, H. (2003). Relaxed selective pressure on an essential component of pheromone transduction in primate evolution. Proceedings of the National Academy of Sciences 100, 3328-3332.

Liman, E. R., and Dulac, C. (2007). TRPC2 and the molecular biology of pheromone detection in mammals. TRP ion channel function in sensory transduction and cellular signaling cascades 2007, 45-53.

Marchand, J. E., Yang, X., Chikaraishi, D., Krieger, J., Breer, H. and Kauer, J.S. (2004). Olfactory receptor gene expression in tiger salamander olfactory epithelium. Journal of Comparative Neurology 474, 453-467.

Martof, B. (1962). Some aspects of the life history and ecology of the salamander *Leurognathus*. The American Midland Naturalist 67, 1-35.

Martof, B., and Rose, F. (1963). Geographic variation in southern populations of *Desmognathus ochrophaeus*. The American Midland Naturalist 69, 376-425.

Mezler, M., Fleischer, J., Conzelmann, S., Korchi, A., Widmayer P., Breer, H., and Boekhoff, A. (2001). Identification of a nonmammalian G_{olf} subtype: functional role in olfactory signaling of airborne odorants in *Xenopus laevis*. The Journal of Comparative Neurology 439, 400-410.

Nakada, T., Hagino-Yamagishi, K., Nakanishi, K., Yokosuka, M., Saito, T. R., Toyoda, F., Hasunuma, I., Nakakura, T., and Kikuyama, S. (2014). Expression of G proteins in the olfactory receptor neurons of the newt *Cynops pyrrhogaster*: their unique projection into the olfactory bulbs. The Journal of Comparative Neurobiology 522, 3510-3519.

Organ, J. (1961). Life history of the pigmy salamander, *Desmognathus wrighti*, in Virginia. American Midland Naturalist 66, 384-390.

Petranka, J. (1998). Salamanders of the United States and Canada. Smithsonian Institution Press.

Pihlstrom, H., M. Fortelius, S. Hemila, F. Forsman, and T. Reuter. 2005. Scaling of mammalian ethmoid bones can predict olfactory organ size and performance. Proceedings of the Royal Society of London B 272, 957– 962.

Pyron, A. R., and Beamer, D. A. (2022). Systematics of the Ocoee Salamander (Plethodontidae: *Desmognathus ocoee*), with description of two new species from the southern Blue Ridge Mountains. Zootaxa 5190, 207-240.

Pyron, A. R., O'Connel, K. A., Lemmon, E. M., Lemmon, A. R. and Beamer, D. A. (2020). Phylogenomic data reveal reticulation and incongruence among mitochondrial candidate species in Dusky Salamanders (*Desmognathus*). Molecular Phylogenetics and Evolution 146, 106751.

Pyron, A. R., O'Connell, K. A., Lemmon, E. M., Lemmon, A. R., and Beamer, D. A. (2022). Candidate-species delimitation in *Desmognathus* salamanders reveals gene flow across lineage boundaries, confounding phylogenetic estimation and clarifying hybrid zones. Ecology and Evolution 12, e8574.

Pyron, A. R., and Beamer, D. A. (2022). Nomenclatural solutions for diagnosing 'cryptic' species using molecular and morphological data facilitate a taxonomic revision of the Black-bellied Salamanders (Urodela, *Desmognathus 'quadramaculatus'*) from the southern Appalachian Mountains. Bionomina 27, 1-43.

Reiss, J. O., and Eisthen, H. (2008). Comparative anatomy and physiology of chemical senses in amphibians. In: Sensory Evolution on the Threshold: Adaptations in Secondarily Aquatic Vertebrates, 43-63.

Różański, J. J., Capillo, G., Lauriano, E. R., Aragona, M., Kuciel, M., Zaccone, G., and Żuwała, K. D. (2020). Ultrastructural and immunocytochemical studies on the olfactory receptor neurons in the *Ichthyosaura alpestris*. Acta Zoologica 102, 437-451.

Sansone, A., Syed, A. S., Tantalaki, E., Korsching, S. I., and Manzini, I. (2014). Trpc2 is expressed in two olfactory subsystems, the main and the vomeronasal system of larval *Xenopus laevis.* Journal of Experimental Biology 217, 2235-2238.

Saint Girons, H., and Zylberberg, L. (1992). Histologie comparée des glandes céphaliques exocrines et des fosses nasales des Lissamphibia. I: Anatomie générale et glandes céphaliques. Annales des sciences naturelles. Zoologie et Biologie Animale 13, 59-82.

Saint Girons, H., and Zylberberg, L. (1992). Histologie comparée des glandes céphaliques exocrines et des fosses nasales des Lissamphibia. II: Epitheliums des fosses nasales. Annales des sciences naturelles. Zoologie et Biologie Animale 13, 121-145.

Schmidt, A., Naujoks-Manteuffel, C., and Roth, G. (1988). Olfactory and vomeronasal projections and the pathway of the nervus terminalis in ten species of salamanders. Cell and Tissue Research 251, 45-50.

Schwenk, K., and Wake, D. B. (1993). Prey processing in *Leurognathu*s and the evolution of form and function in desmognathine salamanders (Plethodontidae). Biological Journal of the Linnean Society 49, 141-162.

Sherman, S. C. (1941). The salamanders of New York. New York State Museum Bulletin 324, 1–365.

Stebbins, R. C., and McGinnis, S. M. (2018). Peterson Field Guide to Western Reptiles & Amphibians. University of California Press.

Strotmann R., Schröck K., Böselt I., Stäubert C., Russ A., and Schöneberg T. (2011). Evolution of GPCR: change and continuity. Molecular and Cellular Endocrinology 331, 170-178.

Syed, A. S., Sansone, A., Hassenklöver, T., Manzini, I., and Korsching, S. I. (2017). Coordinated shift of olfactory amino acid responses and V2R expression to an amphibian water nose during metamorphosis. Cellular and Molecular Life Sciences 74, 1711-1719.

Syrovatkina, V., Alegre, K. O., Dey, R., and Huang, X. (2016). Regulation, signaling and physiological functions of G-proteins. Journal of Molecular Biology 428, 3850-3868.

Thewissen, J. G. M., and Nummela, S. (2008). Sensory evolution on the threshold: adaptations in secondarily aquatic vertebrates. University of California Press.

Venkatachalam, K., and Montell, C. (2007). TRP channels. Annual Review of Biochemistry 76, 387-417.

Wakabayashi, Y., and Ichikawa, M. (2008). Localization of G protein alpha subunits and morphology of receptor neurons in olfactory and vomeronasal epithelia in Reeve's Turtle, *Geoclemys reevesii*. Zoological Science 25, 178-187.

Weiss, L., Manzini, I., and Hassenklöver, T. (2021). Olfaction across the water–air interface in anuran amphibians. Cell and Tissue Research 383, 301-325.

Wake, D. B. (2012). Taxonomy of salamanders of the family Plethodontidae (Amphibia: Caudata). Zootaxa 3484, 75–82.

Wilder, I. W. (1913). The life history of *Desmognathus fusca*. The Biological Bulletin 24, 251-292.

Wilder, I. W. (1925). The morphology of amphibian metamorphosis. Smith College, 6.

Wilson, L. (1995). The land manager's guide to the amphibians and reptiles of the South. The Nature Conservancy.

Wirsig-Wiechmann, C. R., Houck, L. D., Feldhoff, P. W., and Feldhoff, R. C. (2002). Pheromonal activation of vomeronasal neurons in plethodontid salamanders. Brain Research 95, 335-344.

Yildirim, E., and Birnbaumer, L. (2007). TRPC2: Molecular biology and functional importance. Handbook of Experimental Pharmacology 179, 53-75.

Zufall, F., Ukhanov, K., Lucas, P., Liman, E. R., and Leinders-Zufall, T. (2005). Neurobiology of TRPC2: From gene to behavior. Pflügers Archiv - European Journal of Physiology 451, 61-71.

APPENDICES

Appendix A. *Detailed information on specimens used for this thesis research.*

Species	**ID Number**	**Collection Date**	**Euthanasia Date**	**Days spent in lab before euthanasia**	**Snout-vent length (mm)**	**Life stage (larva, juvenile, adult)**	**Sex**	**Technique**
D. amphileucus	JOR-21-039	22 June 2021	14 November 2022	510	95	Adult	Unknown	MicroCT scanning
D. amphileucus	JOR-21-104	25 May 2022	8 March 2023 (found dead)	283	70	Adult	Female	Standard histology
D. amphileucus	JOR-21-113	2 June 2022	12 May 2023	355	31	Larva	Unknown	ISH
D. amphileucus	JOR-21-185	6 June 2022	12 May 2023	336	28	Larva	Unknown	ISH
D. amphileucus	JOR-21-254	8 August 2023	10 August 2023	2	82	Adult	Female	RNA extraction
D. amphileucus	JOR-21-255	9 August 2023	10 August 2023	1	70	Adult	Male	ISH
D. aureatus	JOR-21-141	5 June 2022	24 September 2022	109	53	Adult	Unknown	MicroCT scanning
D. aureatus	JOR-21-141	5 June 2022	24 September 2022	109	53	Adult	Unknown	Standard histology
D. aureatus	JOR-21-142	5 June 2022	23 January 2023	228	33	Adult	Male	ISH
D. aureatus	JOR-21-144	5 June 2022	12 May 2023	337	25	Larva	Unknown	ISH
D. aureatus	JOR-21-147	5 June 2022	14 November 2022	159	28	Larva	Unknown	MicroCT scanning
D. aureatus	JOR-21-147	5 June 2022	14 November 2022	159	28	Larva	Unknown	Standard histology

Species	**ID Number**	**Collection Date**	**Euthanasia Date**	**Days spent in lab before euthanasia**	**Snout-vent length (mm)**	**Life stage (larva, juvenile, adult)**	**Sex**	**Technique**
D. ocoee	JOR-21-046	16 August 2021	1 June 2022	286	54	Adult	Male	RNA extraction
D. ocoee	JOR-21-100	23 May 2022	23 January 2023	240	39	Adult	Male	Standard histology
D. ocoee	JOR-21-126	4 June 2022	5 July 2023	395	26	Adult	Male	ISH
D. wrighti	JOR-21-138	4 June 2022	23 December 2022	200	43	Adult	Unknown	MicroCT scanning
D. wrighti	JOR-21-192	9 June 2022	15 May 2023 (found dead)	371	23	Adult	Unknown	Standard histology
D. wrighti	JOR-21-194	9 June 2022	13 June 2023	369	22	Adult	Unknown	ISH
D. wrighti	JOR-21-271	7 August 2023	10 August 2023	3	23	Adult	Male	RNA extraction
E. eschscholtzii	JOR-21-060	1 October 2021	1 October 2021	0	56	Adult	Female	Standard histology
E. eschscholtzii	JOR-21-061	5 October 2021	5 October 2021	0	42	Adult	Male	RNA extraction
E. eschscholtzii	JOR-21-089	19 April 2022	19 April 2022	0	56	Adult	Female	MicroCT scanning
E. eschscholtzii	JOR-21-243	5 July 2023	5 July 2023	0	56	Adult	Female	ISH
E. eschscholtzii	JOR-21-282	9 October 2023	9 October 2023	0	91	Adult	Male	ISH
P. shermani	JOR-21-054	18 August 2021	18 April 2022	240	57	Adult	Female	RNA extraction
P. shermani	JOR-21-056	18 August 2021	17 January 2022 (found dead)	120	55	Adult	Female	Standard histology
P. shermani	JOR-21-135	4 June 2022	13 June 2023	374	26	Juvenile	Unknown	ISH

Species	**ID Number**	**Collection Date**	**Euthanasia Date**	**Days spent in lab before euthanasia**	**Snout-vent length (mm)**	**Life stage (larva, juvenile, adult)**	**Sex**	**Technique**
P. shermani	JOR-21-261	8 August 2023	10 August 2023	2	18	Juvenile	Unknown	ISH
P. shermani	JOR-21-262	8 August 2023	10 August 2023	2	24	Juvenile	Unknown	MicroCT scanning
P. shermani	JOR-21-262	8 August 2023	10 August 2023	2	24	Juvenile	Unknown	Standard histology

Appendix B. *Primers, reaction conditions and cycling temperatures used to amplify the four different gene fragments from the cDNA of the focal taxa.*

Gene	**Primers**	**Volume of cDNA used[A]**	**Cycling parameters**	**Fragment size (bp)**	**Species**	**Reference**
$G\alpha_{olf}$	5'-GTGACCATAGTTTCAGCAATG-3' 5'-TGCATYCKCTGGATGATGTC-3'	0.7 µl	95°C for 2 min 35 cycles (95°C for 30 sec, 54.5°C for 30 sec, 72°C for 40 sec) 72°C for 5 min	~900	All	Wakabayashi and Ichikawa (2008)
$G\alpha_{o}$	5'-ATYATCCAYGARGATGGHTTCTC-3' 5'-GCRTCRAANACMAMCTGGAT-3'	1 µl	95°C for 2 min 30 cycles (95°C for 30 sec, 53°C for 1 min, 72°C for 1 min) 72°C for 5 min	~850	All	This study
$G\alpha_{i2}$	5'-ATGGGMTGYACHCTGAGCGC-3' 5'-CAGGTTRTTYTTGATGATGAC-3'	1 µl	95°C for 2 min (95°C for 30 sec, 54°C for 30 sec, 72°C for 1 min) 72°C for 5 min	~900	All	This study
TRPC2	5'-TGNCTYAAYCTGKCCATCCG-3' 5'-TCTGRTTYCGGCACATKCCCAG-3' 5'-GTGGCHGTGGACACMAACCA-3' 5'-TCTGRTTYCGGCACATKCCCAG-3' 5'-GTGGCHGTGGACACMAACCA-3' 5'-TAVGGSACRTAGATRTTGTTGA-3'	0.7 µl	95°C for 2 min (95°C for 30 sec, 54°C for 30 sec, 72°C for 1.25 min) 72°C for 5 min	~600 ~500 ~1400	*E. eschscholtzii* *Desmognathus* *P. shermani*	This study This study Kiemnec-Tyburczy et al. (2012)

[A]all other reagent concentrations were identical for all PCRs (25 µl total volume): 1X Green Dream Master Mix (ThermoFisher Scientific) and 2 µM of forward and reverse primers.